

Combining LiDAR and Allometric/Volumetric Equations to estimate Above Ground Biomass from an Airborne LiDAR Scanning Model converted by Terrestrial Laser Scanning Point Cloud

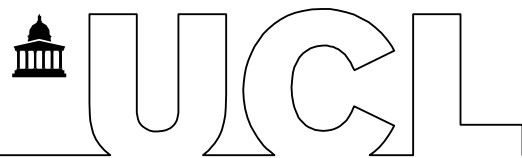


Yuchen Guo

Supervised by Dr Mathias Disney

2018

This research dissertation is submitted for the MSc Remote Sensing at University College London.



DEPARTMENT OF GEOGRAPHY

M.Sc. in Remote Sensing

Please complete the following declaration and hand this form in with your M.Sc. Research Project.

I,Yuchen Guo.....

hereby declare :

- (a) that this M.Sc. Project is my own original work and that all source material used is acknowledged therein;
- (b) that it has been prepared specially for the MSc in Remote Sensing of University College London;
- (c) that it does not contain any material previously submitted to the Examiners of this or any other University, or any material previously submitted for any other examination.

Signed :Yuchen Guo.....

Date : August 2018.....

Abstract

Calculating the AGB by combining active remote sensing with allometric equation has been widely used to comprehend carbon storage in the terrestrial ecosystems. ALS regarded as a relatively accurate and easy to obtain data become a popular active remote sensing data source for AGB estimation. However, using ALS point cloud with allometric or volumetric equations to generate the AGB has a large bias with the actual value and need to be validated as well as calibrated for further study.

In general, as the destructive method cannot be applied to validate the method, TLS estimation replaced the destructive method as the reference. To decrease this bias, in this project, a ALS model was converted by TLS is applied to decreased bias brought by the ALS point cloud, like the ALS point cloud cannot perfectly match the TLS point cloud especially in the boundary area. The ALS model build in this project, perfect match resource TLS point cloud according compared the ALS point cloud and TLS point cloud.

Basing on the relatively accurate ALS model, this project also tests three kinds of methods for AGB estimation (species-specific and plot area allometric equation as well as volumetric equation). Evaluating the uncertainty and bias of each equation and discussing the uncertainty and bias from the ALS model and process of calculating the AGB. From the result and discussion, the bias and uncertainty factors are from the growth characteristic of high density woodland, the crown selection in TLS, CP to DBH, tree segmentation parameters, species link from ALS to TLS, DBH for allometric equation as well as height and DBH for volumetric equation. According to comparing three methods of estimating the AGB (Figure 15), species-specific allometric equation is the most valid method to estimating the AGB regardless of the Hawthorn which takes up 63.215% of the reality AGB because the AGB calculated by plot area allometric equation is not satisfied comparing with the other two methods and the ALS AGB calculated by volumetric equation are two low comparing with TLS AGB. To gain a relative accurate AGB by using the method in this project, the method of generating DBH and species geo-referencing are highly recommended to be improved in the future work.

Acknowledgements

Firstly, I would like to give my deepest gratitude to my supervisor Dr. Mathias Disney for his guidance, encouragement and constant support throughout the duration of my project and recommend me to others. I would like to express my greatest appreciation of his advices on all the stages of finishing my dissertation.

Secondly, my gratitude is also extended to Jonathan Williams for giving me the support on the knowledge of Tree crown delineation as well as relevant knowledge.

Also, my great appreciate to Kim Calder for data supporting and Tom knight's supporting in UNIX

My sincere gratitude also goes to Hamraz, H., M.A. Contreras, and J. Zhang for supporting me the research Library for segmenting individual trees within LiDAR point clouds in python to delineate individual tree, although we never talk.

Yuchen, Guo

August 2018

List of contents:

Page:

1. Introduction	10
1.1 Background	10
1.2 Problem Statement	10
1.3 Research aim and Objectives	11
1.3.1 Research Aim	11
1.3.2 Objectives	11
2. Literature Review	12
2.1 Field measurement to estimate the AGB	12
2.2 Allometric equation to estimate the AGB	13
2.3 Remote sensing to estimate the AGB	14
2.3.1 Passive sensor	14
2.3.2 Active sensor	15
3. Materials and methodology	16
3.1 Study site	16
3.2 ALS Dataset	17
3.3 TLS Dataset	18
3.4 Methodology	19
3.4.1 Converting the TLS to ALS	20
3.4.2 Tree segmentation code	21
3.4.3 Species geo-referencing	22
3.4.4 From the Crown Perimeter to DBH	22
3.4.5 Allometric equations to estimate the AGB	23
3.4.5 Volumetric equations to estimate the AGB	24
4. Results	25
4.1 ALS (convert by TLS)	25

4.2 Ground and vegetation area extraction.....	28
4.3 From crown perimeter (CP) to diameter at the breast height (DBH)	29
4.4 Tree segmentation.....	30
4.5 Tree species geo-referencing	31
4.6 AGB estimation	32
4.6.1 Species-specific allometric equation	32
4.6.2 Plot area allometric equation	34
4.6.3 Volumetric equation	35
5. Discussion	37
5.1 Discussion about ALS model.....	37
5.2 Discussion on the crown perimeter (CP) to DBH	38
5.3 Discussion on tree species geo-referencing	39
5.4 Discussion on tree segmentation results	39
5.5 Discussion on results of estimated AGB.....	42
5.5.1 Discussion on species-specific allometric equation.....	42
5.5.2 Discussion on plot area allometric equation.....	42
5.5.3 Discussion on volumetric equation.....	43
5.6 Discussion the limitation and implication	43
6. Conclusion.....	45
7. Auto-Critique	46
8. References	47
9. Appendices	52

List of Figure:

Figure 1. The location of 1-hectare study site (red bounding box) in Wytham Woods, UK	(17)
Figure 2. The ALS (A) point cloud and TLS (B) individual tree point cloud of 1-hectare study site (red bounding box) in Wytham Woods, UK	(18)
Figure 3. The flow chart of methodology to generate ALS model and estimate the AGB and evaluate the uncertainty and bias	(19)
Figure 4. The location percentage of each tree crown of 559.	(26)
Figure 5. Visual flow chart of generating the ALS model from individual TLS tree point cloud.	(27)
Figure 6. Cloud compared result between ALS model and ALS.	(28)
Figure 7. Cloud compared result between ALS model and TLS point cloud.	(28)
Figure 8. Cloud compared result between ground point from ALS model and DEM point cloud.	(29)
Figure 9. Linear Regression of CP and DBH, which statistics from 559 TLS point cloud trees and LeafData_3Dmodel_metadata.xlsx	(30)
Figure 10. The position of all ALS tree tops and TLS trees corresponded with ALS trees as well as all 559 TLS' s position with species	(31)
Figure 11. Linear Regression between TLS tree height(H_{re}) and ALS tree height (H_{ca}) (blue) as well as the relationship between TLS tree height and ALS tree height in	

theoretical and threshold of 1m and 5m (red).

..... (37)

Figure 12. the layout of 559 TLS trees' crowns in the top view, which generated by OpenCV in python (Appendix A)

..... (40)

Figure 13. tree segmentation result derives from ALS model (NOMINAL_POST_SPACING = 0.85)

..... (41)

Figure 14. tree segmentation result derives from ALS model (NOMINAL_POST_SPACING = 0.5)

..... (41)

Figure 15. tree segmentation result derives from ALS model (NOMINAL_POST_SPACING = 0.3)

..... (41)

Figure 16. Bar chart of total AGB estimation from different allometric and volumetric equations; ALS1/TLS1 represent all species without unidentified trees and ALS2/TLS2 represent all species without Hawthorn and unidentified trees

..... (45)

List of Table:

Table 1. Different parameters based on species in the study site

..... (25)

Table 2. Varied species wood density in the study site

..... (25)

Table 3. AGB estimation from species-specific allometric equation derive from TLS tree point clouds

..... (33)

Table 4. AGB estimation from species-specific allometric equation derive from ALS model

..... (33)

Table 5. AGB estimation from plot area allometric equation derive from TLS tree point cloud model

..... (34)

Table 6. AGB estimation from plot area allometric equation derive from ALS model

..... (35)

Table 7. AGB estimation from volumetric allometric equation derive from TLS tree point cloud

..... (36)

Table 8. AGB estimation from volumetric equation derive from ALS model

..... (36)

Table 9. Rescale AGB from three methods: (1) AGB derives from species-specific allometric equation.

..... (44)

1. Introduction

1.1 Background

Biomass is an industry term to measure the burning wood as well as other organic matter's energy (Demirbaş, A., 2001). It has strong coherent with the carbon emission, which is regarded as a crucial parameter when scientists make research in the field of various terrestrial carbon studies (Solomon et al., 2009; IPCC, 2014). According to the IPCC (2014), the biomass can also be divided into above-ground biomass, below-ground biomass, the dead mass of litter, woody debris and the soil organic as different carbon pools (Vashum, K.T. and Jayakumar, S., 2012). Among the above five parts of biomass, above-ground biomass is regarded as the most important and visible carbon pool of the terrestrial forest ecosystem.

To gain above ground biomass (AGB), the scientists in the relevant field generate many methods, such as destructive method, allometric equation method remote sensing method etc. In those methods, the most accurate one is through measuring the oven-dried weight of cutting tree, however, due to the destructiveness, time-consuming this method cannot be extensive used. However, it can be used to validate other methods. Allometric equation method is also widely used in AGB estimation by building the relationship between different biophysical parameters and AGB or volume (Ravindranath, N.H. and Ostwald, M., 2008, Lu, D.,2006), however due to involving large amount of field work, it is still a impractical method applying in large scale area.

As the developing of remote sensing, more and more remote sensing methods are involved in estimating the AGB combining with active remote sensing due to its ability to capture the biophysical parameters remotely and extensively.

Light Detection and Ranging (LiDAR) as an active is remote sensing method widely used method to gain a relatively accurate canopy point cloud model due to its capability of gaining high resolution vegetation profile nor matter in airborne laser scanning (ALS) or terrestrial laser scanning(TLS) (Gibbs et al., 2007).

1.2 Problem Statement

As LiDAR scanners to estimate the AGB, no matter terrestrial laser scanning (TLS) or

airborne laser scanning (ALS), they all could characterize the vertical canopy structure for individual tree to a plot area (Tang et al., 2012). However, it is impossible that they can gain the complete forest structure, especially for the ALS. In most cases, only vertical scan results are available which are provided by ALS. Compared with ALS, TLS furnishes more precise scan results and contributes more in the understory part (Liu et al., 2017). Researchers use the TLS scanning results rebuild the quantitative 3D tree models via various algorithms (Seidel et al., 2012; Raunonen et al., 2013; Bournez et al., 2017). However, although the TLS has so many advantages both in precise and information, it cannot apply into large area due to the time-consuming as well as large amount of field work (Newnham et al., 2015). Therefore, using ALS dataset to estimate the AGB value becomes a more efficient and feasible method to be applied. According to current situation, ALS data have already been used in roughly acquiring forest structure information and the results always present in a very low accuracy (Lim & Treitz, 2004). Hence, an effective and accurate ALS data estimating method in a large plot level is imperatively acquired. What's more, to generate a fine estimating method, A simulated ALS model which can be verify is highly needed.

1.3 Research aim and Objectives

1.3.1 Research Aim

The main research aim of this study focuses on ALS model built by TLS point cloud of 1 hectare in Wytham Woods, UK and the AGB (Above Ground Biomass) estimation from ALS model by using allometric and volumetric equations as well as evaluating the uncertainty and bias of the ALS model and methods used in this project.

1.3.2 Objectives

- Identifying each TLS tree's upper crown area and root area.
- Merging the upper crown area point cloud and root point with local DEM.
- Using Rasterize in Z direction (CloudCompare) to generate a ALS point cloud model.
- Editing and deleting invalid point cloud from ALS point cloud model which converted by TLS.
- Comparing the ALS model with ALS and TLS data in same area
- Extracting the ground points and off-ground points from ALS model by using

CloudCompare.

- Tree segmentation by using Python and statistics each segmented tree's biophysical parameters (Height and Crown perimeter (CP) and the coordinate of the tree top).
- Generating the correlation between diameter at breast height (DBH) and CP
- Registering the ALS trees with TLS trees
- Estimating the AGB by applying species-specific or plot level allometric equation as well as volumetric equations from the ALS model and evaluating the uncertainty and bias of the results

2. Literature Review

Estimating the above-ground biomass is regarded as a vital important research in the study of the terrestrial forest ecosystem pools (Vashum, K.T., Jayakumar, S., 2012). The practitioners generate many methods to calculate the AGB. According to relevant research paper, there are roughly three methods using to estimate the above-ground biomass (AGB) in the forest, which are field measurement, remote sensing as well as GIS methods (Anaya, J.A, et al., 2009). In this section, each AGB estimation method will be presented.

2.1 Field measurement to estimate the AGB

The field measurement can be divided into destructive method and non-destructive. The destructive method, also known as harvest method, is regarded as the most intuitive method for estimating the biomass of vegetations the harvest method's main step is harvesting all known tree components at first and then classify those components, such as branches, leaves and trunk and measuring the weight of each components as well as weight the oven dried components. It might be the most accurate method to estimate the above-ground biomass, however, due to the complex and time-consuming field operations, it can be only measure small sample sizes or a small area. What's more, for some degraded forest or some forest habitat containing rare species, the harvest method is highly not recommend or prohibited because of

the destructive feature. However, it can be used as a method to validate other methods (Nordh, Verwijst., 2004; Devi, Yadava., 2009). As for the non-destructive method, it can solve the problem when there are protected and rare tree species existing in the ecosystem and destructing them might bring unpractical and unfeasible results (Montes et al., 2000). For example, the study in thuriferous juniper woodland which located in the High Central Atlas, South of Morocco, apply the non-destructive method to calculate the biomass. The main detail of this method is counting the tree shape (taking two orthogonal angles' photographs) and sampling the tree components of different components (branches, leaves, drunk etc.) and calculating each component's volume and bulk density (Brown et al., 1989). Except for the sampling measurement, another way of non-destructive is applying the allometric equation by measuring each tree' height, diameter at breast height (DBH), as well as volume of the tree and wood density. This method also involves lots of fieldwork which means large amount of human cost.

2.2 Allometric equation to estimate the AGB

Linking the AGB or volume with different biophysical parameters of trees has been wildly applied in allometric equation field in diverse kinds of forests. For the tropical rainforest, due to its huge coverage among the globe, the allometric equation has been developed abundant. In 1997, brown modified several allometric equations for broadleaf forests based on different zones from dry, moist to wet and analyzed the accuracy of the allometric equation equations. As more and more tree dataset has been obtained from the field work, more and more allometric relationship has been established in the tropical area. according to different rainforest type in Brazil, central Amazon forest and Indonesian Borneo, those areas' allometric equations are established ((Araújo et al., 1999; Hashimoto et al., 2000; Chambers et al., 2001).). From the processing of the allometric equations' model building, scientists find that the large trees contribute a relatively larger bias in allometric equation when estimating the AGB. Meanwhile, estimating the AGB based on the allometric equations involve lots of field measurement, hence, it also has the limits for those regression models to build a large area plot or full tree species. To solve above issues, Chave et al built regression allometric equation coherent with several parameters (woody density, tree height, trunk cross-sectional area) to estimate the biomass in 2005, which can be used

to predict AGB in a broad range of tropical forest. According to the result, the tropical forests which are in the secondary or the mature give the uncertainty of 0.5 – 6.5% due to the overestimates prevailed. Height is a crucial variable to reduce the overestimate, but with the height involve, the regression error increase at the same time (Hunter et al., 2013). To minimize bias, in 2015, Chave et al developed more about diameter-height relationship to improve the allometric equation and the accuracy of biomass assessment protocols in tropical vegetation types.

Wytham woods which is this project's study area is regarded as a significant important site for studying allometric equation in UK and other European countries. Since 1992 the Environmental Change Network (ECN) had already started measuring the local trees' diameter at the breast (DBH) and height for the standard protocols and in 2008 as well as 2010 the DBH's of the trees were updated by Malhi and Butt. There are mainly 5 species of tree growing in the Wytham woodland which are Ash, Birch, Oak, Sycamore and Lime according to the statistics. Since 1968, Bunce started to make a propose that correlations between oven-dries weight of trees and DBH among above species (in \log_e terms). From the report, the uncertainty for these species-specific trees is relatively low with R^2 range from 97.4% to 99.5%. What's more, for the common hawthorn (*Crataegus monogyna*), only a relative allometric equation for estimating AGB of hardwoods located at four study sites in Pennsylvania state, US was found to apply in Wytham woods. According to the research, R^2 for this allometric equation is 0.85 and the average bias is 90.05 (Dickinson & Zenner, 2010). Addition to allometric equations for individual species-specific trees, Randle et al. (2014) revised allometric equations to make them reasonable for estimating AGB at area level. They reclassified the species into several species group to apply the functions and divided the estimation into three subsequent equations based on the size of DBH. Although these revised equations are difficult to validate using destructive approach, they are widely used in UK to estimate AGB at larger scale

2.3 Remote sensing to estimate the AGB

Remote sensing method can be divided into passive and active according the energy source which are both widely used in estimate the AGB in forest.

2.3.1 Passive sensor

Passive remote sensing acquires the information from nature energy like the visible,

near-infrared as well as the thermal infrared parts of the electromagnetic spectrum. Based on the different resolution passive sensor, they apply different methods to estimate the biomass. For the fine spatial-resolution which spatial resolution are less than 5 m, the data source could be aerial photographs, space borne or airborne, such as IKONOS, QuikBird and many approaches have been used to extract the biomass parameters (tree height, crown diameter, crown closure and stand area) through the fine resolution data, which include bottom-up algorithm, top-down algorithm as well as template matching (Culvenor, 2003). For example, Thenkabail et al used IKONOS data to estimate AGB of oil palm plantations in Africa. For the medium spatial-resolution data which spatial-resolution ranges from 10 to 100 m. the most frequently used in medium spatial-resolution should be time-series Landsat data, which can estimate the AGB at local and regional scales. According to the previous work, the AGB can be estimated by using medium spatial-resolution data through different methods from regression analysis, k-nearest neighbors to neural network (Lu., 2005; Tian,X, et al.,2012; Anaya, J.A. et al., 2009). As for the Coarse spatial-resolution data, which spatial resolution is over than 100. The main coarse spatial-resolution include NOAA Advanced Very High-Resolution Radiometer (AVHRR), SPOT VEGETATION, and Moderate Resolution Imaging Spectroradiometer (MODIS). Those data are used to estimate the AGB in national, continental as well as globe scale. For example, the AVHRR NDVI data were used to estimate biomass density and assess burned areas, burned biomass, and atmospheric emissions in Africa (Barbosa, P. M., Stroppiana, D. and Gregoire, J. 1999.).

2.3.2 Active sensor

In some area of the earth, there are frequent cloud conditions restraining the acquisition of passive remote sensing data. Thus, the Active remote sensing is regarded as a method with less influenced by environment are applied to solve this problem. Based on the data variety, active remote sensing can be divided into radar and lidar data. For radar, due to its feature that it can collect Earth feature data irrespective of the weather and light conditions, the radar data has been extensively used in AGB estimation. Different radar data have their own characteristic in connecting with biophysical parameters. For example, radar backscatter in the P and L bands is highly correlated with major forest parameters, such as tree age, tree height, DBH, basal area, and AGB (Lu, D., 2006). L-band backscatter is suitable for estimating

biomass of regenerating forests in tropical regions (Austin, J. M., Mackey, B. G. and van Niel, K. P. 2003). From the previous research, they indicated that long-wavelength radar data have the advantages in AGB estimation for complex forest stand structure. For LiDAR, it can be divided into TLS and ALS. TLS is regarded as a relative accurate method to estimate the AGB, the quantitative structure models of single trees from Laser Scanner Data are generated to gain a thorough biophysical parameter from TLS (Åkerblom, M., Raumonen, P., Mäkipää, R. and Kaasalainen, M., 2017; Calders, K., et al). However, TLS cannot apply into large scale area due to its high consuming in Time and money. According to the current situation, it can be used as a validate reference for some study area. ALS is used for estimating biophysical parameters (Næsset, E., Bollandsas, O. M. and Gobakken, T. 2005) by using airborne laser as well as lidar systems, such as height, DBH, crown area and volume and combine with allometric equation to estimate the AGB. According to the laser scan resource of forest, the lidar point can divided into area-based approach and tree-centric approach. The first one is calculating the AGB in plot area, but it can only apply in some specific area. As the second model is more appealing due to it can sum the biomass of individual trees (Coomes, D.A., 2017). In this way, if knowing the species allometric equation, the accurate AGB could be calculated. However, using the tree-centre model involves in registering tree species by applying individual tree's allometric equation. Hence if a fine individual tree allometric equation is calibrated, it is necessary to use an accurate ALS to validate tree-centric approach.

3. Materials and methodology

3.1 Study site

The study area is located at Wytham Woods, Oxford, UK ($1^{\circ}20'W, 51^{\circ}47'N$; Figure 1). The study of this place began in 1943 for the forest ecosystem. After over half a century research, this area has become a globe leading research sites and could fulfill to quantify the uncertainty of ALS as well as TLS among diverse levels, because the data from airborne LiDAR and terrestrial LiDAR as well as the species of this area has already been sufficiently covered. In this research, to calculate the AGB and evaluate the uncertainty of the results, there are two solutions could be applied which are from ALS dataset and TLS dataset respectively.

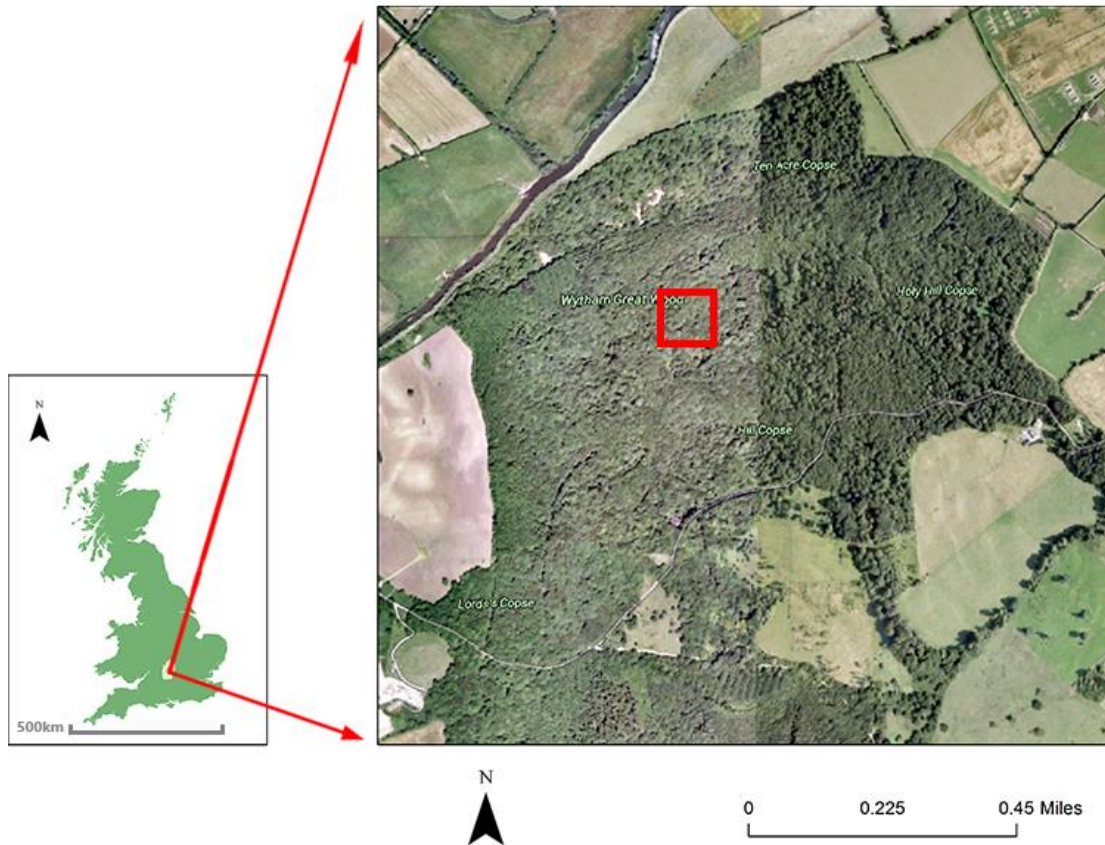


Figure 1. The location of 1-hectare study site (red bounding box) in Wytham Woods, UK

3.2 ALS Dataset

The ALS dataset (Figure 2, A) of the study area (Wytham Woods) was generated by Coomes on 24th June 2014 through RG13_08 Airborne Research and Survey Facility (ARSF). The horizontal datum is projected with OSGB36 and the vertical datum is Newlyn and British National Grid projection. According to the ARSF, the data has already been pre-processed which is a basic noise-cleared point clouds file. From the Cloud-Compared window interface or other visual interface, the ALS dataset is an around 4 hectare point cloud. It is the 1-hectare sample site with a 50 m buffer of each side which cover the whole study area. Farther more, from the DEM extracted by CSF in CloudCompare, it illustrates that the terrain of the study site gradually increases from NW to SE, which range is from -29.386m at the northwest to 4.3735m at southeast, about. The point density is 7.14 per m² and the point space is 0.37 m. The whole area contains 306537 returns points which format are X, Y and Z. In this project,

the ALS point cloud is used to compared with the ALS (convert by TLS). Hence, the project will not display and discuss in detail.

3.3 TLS Dataset

The TLS data can be divided into two parts, the first part is 559 individual trees named by their serial numbers (Figure 2, B). They have txt and pcd two kinds of formats which contain X, Y and Z information. Another part is a xlsx file named “LeafData_3Dmodel_metadata.xlsx” (Appendix B). In this xlsx file, it contains Tree ID, species, coordinates, volume, height and DBH if 559 individual trees in the 1-hectare central study area. According to the work from Calders (2017), those individual TLS tree data are acquired by RIEGL VZ-400 terrestrial laser scanner and highly processed to tree point cloud without noise.

According to the statistic from the TLS dataset, there are 386 Sycamore (*Acer pseudoplatanus*), Taxonomic code as ACERPS; 2 Field maple (*Acer campetre*), Taxonomic code as ACERCA; 35 Common hazel (*Corylus avellana*), Taxonomic code as CORYAV; 19 Common hawthorns (*Crataegus monogyna*), Taxonomic code as CRATMO; 52 European ash (*Fraxinus excelsior*), Taxonomic code as FRAXEX, 24 Pedunculate oak (*Quercus robur*), Taxonomic code as QUERRO; as well as 41 unknown species trees.



Figure 2. The ALS (A) point cloud and TLS (B) individual tree point cloud of 1-hectare study site (red bounding box) in Wytham Woods, UK

3.4 Methodology

To calculate and evaluate the uncertainty of the AGB by using ALS, the ideal method is to register the ALS with TLS as accurate as possible. however, it is hard to achieve the result that two point-clouds matched perfectly in spatial because it is hard and impractical to find feature points. In this research, it applies a solution which is extracting the canopy point as well as root point from the TLS tree point cloud and simulate ALS data, then estimate the AGB by utilizing ALS model which converted by TLS.

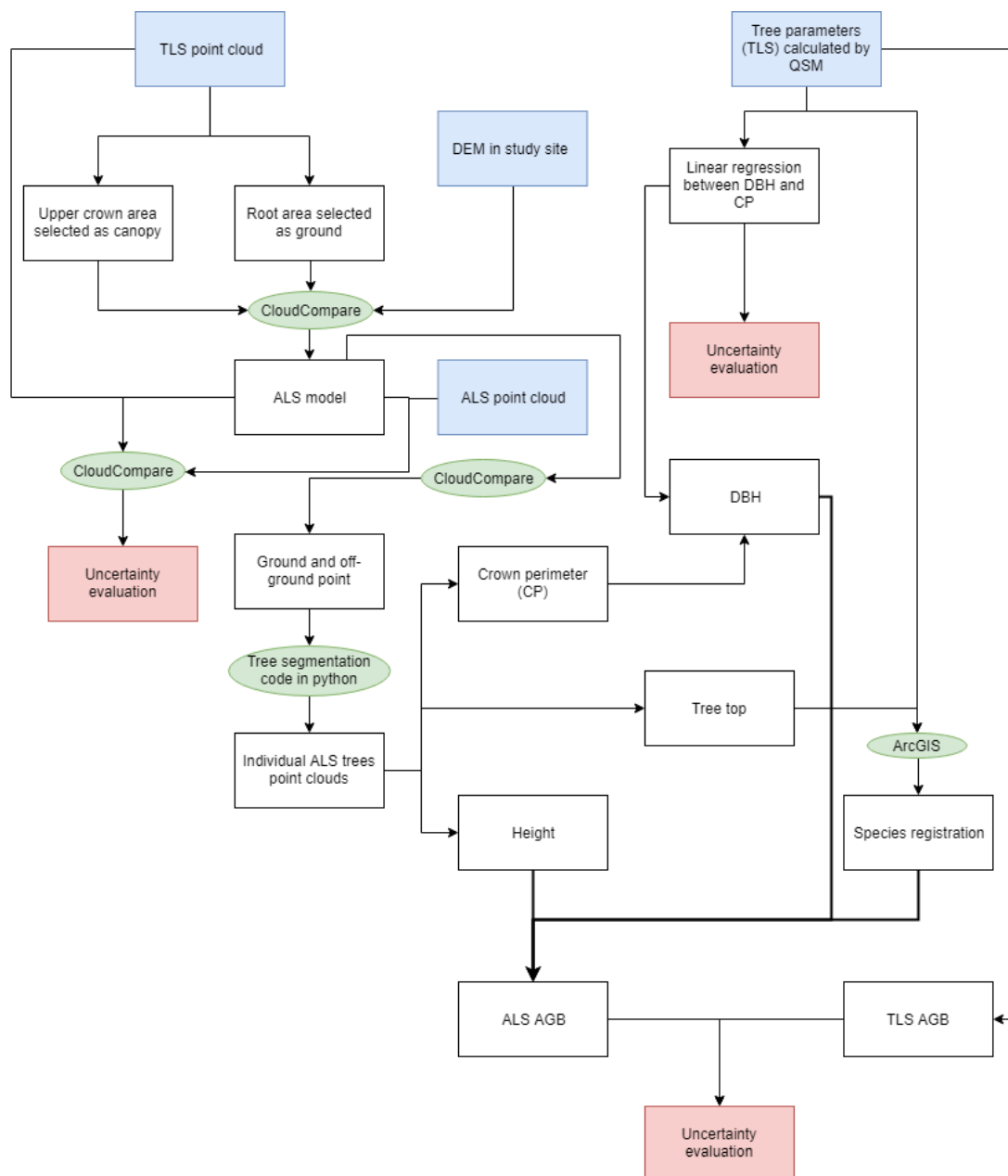


Figure 3. The flow chart of methodology to generate ALS model and estimate the AGB and evaluate the uncertainty and bias

The methodology of calculating the above ground biomass can be divided into the following steps: Selecting upper crown area as well as root area from individual trees point cloud; Merging all point cloud with local DEM; Generating ALS model; the Extracting the ground point and off-ground point by using Cloth Simulation Filter (CSF) in CloudCompare; Reclassifying the ALS point cloud and normalizing the intensity of each point in python; Delineating the tree segmentation by using the code supported by Hamid Hamraz,2016 in python; Gathering the trees' parameters; linking the ALS trees (convert by TLS) with TLS trees and calculating the AGB and qualifying the uncertainty and bias(Figure 3).

3.4.1 Converting the TLS to ALS

ALS data which is used in this project is acquired from overhead angle. Hence, the information from the ALS contains the canopy of the vegetation and ground area without vegetation covered. As for the TLS dataset, they contain more information about the trees including the canopy, the shape of the trunk, the DBH as well as height of individual trees. To gain the similar point cloud as ALS from the TLS. The valid dataset which was extract from TLS are upper crown area for canopy and root area for ground. Since there is no ground information in TLS, the TLS dataset covers where the root area located which can be used to simulate the ground area. To gain high density ground point, the local DEM can be applied to merge into extraction point cloud. Hence, the entire process of converting TLS to ALS is in the below steps: extracting the upper crown area from each individual tree of 559 as well as the root area by using python. Merging all the selected point clouds into 1 point-cloud by using python. Merging the canopy-root point cloud with local DEM by using CloudCompare. Generating ALS point cloud by using Rasterize tools in CloudCompare. According to parameter setting, grid step is 0.02 with height grid value. The direction of projection is Z and left the empty value as default. After upgrading the grid, export the mesh as point-cloud. Then we generate the mimetic ALS point-cloud from TLS.

3.4.2 Tree segmentation code

Tree segmentation algorithm is the hardcore of estimating the above-ground biomass by using LiDAR dataset. The code was modified by Hamraz in 2016 which is a robust approach for tree delineation in deciduous forests by using small-footprint airborne LiDAR point-cloud. According to the manual, the code can achieve two kinds of method to delineate the tree segmentation, the first one is A DSM-based method which is applied for the surface data. It is a robust method and can identify most of the dominant, co-dominant as well as intermediate trees with quite high precision. What is more, the overtopped trees can also be recognized by the code. The second method is multi-story, it can layer the point cloud and segment each layer independently by using DSM-based method. In this project, we applied the first method which the `multilayers = 0`. The code is divided into 5 parts which are *util.py*, *geometry.py*, *forest.py*, *crownSegmenter.py* and *constants.py*. In those 5 parts, the basic configuration of the delineation method as well as point cloud parameter can be set in *constant.py*. `NOMINAL_POST_SPACING` is one of most important parameters and should be setting based on the point cloud in advanced (as the manual mentioned, all the length metrics are in feet). Meanwhile, the `MINIMUM_DETECTABEL_CROWN_WIDTH` should be changed at the same time. The value of the `MINIMUM_DETECTABEL_CROWN_WIDTH` should be 4 times of the `NOMINAL_POST_SPACING`, in this way the minimum crown width could be detected. In this project, the `NOMINAL_POST_SPACING` is set as 0.3, hence, as the suggestion, the `MINIMUM_DETECTABEL_CROWN_WIDTH` should be 1.2. Except for the above parameters, other parameters can also be modified if desired. In this project, we change the `MINIMUM_TREE_HEIGHT` to 2.0.

What is more, after changing the parameters of the code, the dataset should strictly follow the format of example dataset. The input point cloud should be save as CSV format with 6 parameters: x, y, z, class, intensity, and return. According to the manual, the point-cloud should be classified as ground and off-ground point. the ground point equal to 2 or 8 and the off-ground point equal to 3, 4, or 5 as the vegetation. Meanwhile, there is at least one ground point to normalize the heights. In this project, we regard all the point cloud as 2 and all the off-ground point (vegetation) as 5.

The result csv file of the segmentation code can be regard as the initial ALS point cloud is segmented into lots of small point cloud. Each point cloud can be regard as

individual tree's point cloud. From each tree point cloud, the height and crown perimeter as well as tree top position can be extracted from the point cloud. The height can be defined as the vertical distance between the highest point and the lowest point. The crown perimeter, which is used to generate the DBH, will be discussed in 3.4.4. The tree top position, which is regarded as the highest point of individual ALS tree point cloud. Initially, no matter the ALS data or the TLS data, they do not give the intensity information. As the format of the data needs to be strictly as the manual given, so the intensity should be normalized according to the height of each point (z), which can be expressed as:

$$\text{Intensity}_z = z \cdot \frac{z}{z_{\max} - z_{\min}} \quad (1)$$

3.4.3 Species geo-referencing

After individual ALS trees are extracted by using tree segmentation code, before applying the allometric equation and volumetric equation to estimate the AGB, each ALS trees should be registered with each TLS trees. From the ArcGIS, the "Near" analysis is applied to register the ALS trees with TLS trees. It is an algorithm which can find the near feature point of ALS tree position from TLS tree position. Consequently, the ALS trees are linked with species.

3.4.4 From the Crown Perimeter to DBH

After applying the tree segmentation code, we got each individual tree's point cloud as well as boundary point. In this project, we regarded the length of boundary as crown perimeter. To gain a suitable relationship between the crown perimeter and diameter at the breast height. From the previous work proposed by Shrivastava and Singh (2003), they generated the relationship between crown diameter (CD) and DBH. According to the research, the DBH and CD are subject to a linear relationship. Hence, the assumption that the relationship between crown perimeter (CP) and DBH are subject to linear relationship can be applied into this project. Corresponding, we statistic the known 559 trees' DBH and CP to generate the relationship between DBH and CP by using linear regression. To generate relatively accurate equation of linear regression. It is better to separate data and generate linear regression equation separately. As the data present, the relationship of the DBH and CP are different when the value of CP is relatively minor compared with the value of the CP is large. Hence, to solve this problem, the CP values are separated by when CP equal 10m. When the

CPs' value is equal or larger than 10 m, the CP and DBH are applied into one linear regression equation and when the CPs' value is less than 10m, another linear regression function is applied. Figure 9 gives the equations of linear regression between CP and DBH.

3.4.5 Allometric equations to estimate the AGB

To estimate the AGB of the study area, this project applies two methods to estimate the AGB:

The first method is using species-specific allometric equations. Before using this kind of allometric equation, it is necessary to link the ALS trees with TLS trees as well as their species. The "Near (Analysis)" algorithm in ArcGIS 10.3 is used to link the ALS trees with the TLS trees. This algorithm can register the tree top of the ALS with the stem of TLS. After the registration, in this project, according different tree-species, different allometric equation are applied.

In the study area, as mentioned previously, there are totally 6 kinds of tree species, which are Sycamore, Field maple, Hazel, Hawthorn, Ash and Oak. Take different allometric equations according to varied species.

For Sycamore:

$$\ln(ABW) = -2.7606 + 2.5189 \cdot \ln(DBH) \quad (2)$$

$$\ln(ABW) = -2.7018 + 2.5751 \cdot \ln(DBH) \quad (3)$$

For European Ash:

$$\ln(ABW) = -2.4598 + 2.4882 \cdot \ln(DBH) \quad (4)$$

$$\ln(ABW) = -2.4718 + 2.5466 \cdot \ln(DBH) \quad (5)$$

For Oak:

$$\ln(ABW) = -2.4232 + 2.4682 \cdot \ln(DBH) \quad (6)$$

$$\ln(ABW) = -2.3223 + 2.4029 \cdot \ln(DBH) \quad (7)$$

$$\ln(ABW) = -3.1404 + 2.8113 \cdot \ln(DBH) \quad (8)$$

$$\ln(ABW) = -3.1009 + 2.6996 \cdot \ln(DBH) \quad (9)$$

where ABW is the Aboveground Biomass for Woodland in kg, and DBH in cm, above species-specific allometric equations are supported by Bunce (1968). For the same species, different allometric equations have different R^2 . Hence, the average ABW of the same species are applied in this project.

As for Common Hawthorn (*Crataegus Monogyna*), the allometric equation is supported by Dickinson and Zenner in 2010. This allometric equation was once used in Hawthorn, Pennsylvania, U.S.A., which is expressed as below:

$$\ln(AGB) = 3.6834 + 2.3405 \cdot \ln(DBH) \quad (10)$$

where DBH is the diameter at the breast height, which unit is cm. According to the research, R^2 for this allometric equation is 0.85 and the average bias is 90.05. For the farther result of the study area, it can be find in the result and discussion sections.

The second method is calculated AGB at plot area. The plot area allometric equations are supported by Randle et al (2014). In the research, they simplified the species. All the Sycamore and Field Maple are regarded as beech; all the common Hazel and Hawthorn, Ash as well as Oak are regarded as Oak. According to the width of the DBH, the research divided the allometric equation into 3 parts, which show the detail allometric equations below:

For $DBH < 7$ cm:

$$AGB = b \cdot DBH^p \quad (11)$$

The unit for AGB is t and for DBH is cm. b as well as p are species parameters: $b_{\text{beech}} < 7 = 0.0001172993$, $b_{\text{oak}} < 7 = 0.0001136009$, while for $p = 2$ in both species.

For $7 \text{ cm} \leq DBH \leq 50 \text{ cm}$:

The allometric equation is the same as when the $DBH < 7$ m, the only difference is the parameters: $b_{7 \leq \text{beech} \leq 50} = 0.0000188154$, $b_{7 \leq \text{oak} \leq 50} = 0.0000168513$, while for $p = 2.4767$ in both species.

For $DBH > 50$ cm:

$$AGB = a + b \cdot DBH \quad (12)$$

As for beech, $a_{\text{beech} > 50} = -0.459518648$, $b_{\text{beech} > 50} = 0.015263082$; while as for oak, $a_{\text{oak} > 50} = -0.41155064$, $b_{\text{oak} > 50} = 0.013669801$

3.4.5 Volumetric equations to estimate the AGB

Volumetric equation is another method to calculate the AGB. In this project, it applies the volumetric equation which is supported by Broadmeadow et al. (2005) to calculate the Sycamore, European Ash and Oak in UK, which is displayed below:

$$Vol = a + b \cdot (DBH)^2 \cdot H^{0.75}$$

Where the Vol is the volume of the tree in m^3 and the unit of the DBH is cm, for H is m. Table 1 illustrates the different parameter based on species, supported by

Broadmeadow et al (2005).

Table 1. Different parameters based on species in the study site

Species	a	b
Sycamore	-0.012668	0.0000737
European Ash	-0.012107	0.0000777
Oak	-0.011724	0.0000765

After gaining the volume of each tree, AGB can be calculated by using volume multiply the wood densities which are offered by the Wood database (2017), Zeidler (2012) as well as Richter & Dallwitz (2000).

Table 2. Varied species wood density in the study site

Species	Woody density (kg/m ³)	References
Sycamore	615	The Wood Database (2017)
Hawthorn	850	Richter & Dallwitz (2000)
European Ash	680	The Wood Database (2017)
Oak	675	The Wood Database (2017)
Hazel	627	Zeidler (2012)

4. Results

In this part, the project will present the results in the following 6 aspects:

4.1 ALS (convert by TLS)

In this project, the ALS point cloud which is used to estimate the AGB is converted by all the individual tree point clouds from TLS. It can be divided into 3 parts (Figure 5): the first part is finding the largest crown place of 559 individual trees in both x direction and y direction as well as roots position of 559 trees (Figure 5; Aa, Ab, Ac). The root

area is defined as all the point among the nadir and 0.01 m above the nadir of each individual tree. It can be regarded as the ground point for simulating the ALS; According to the statistic result, the mean value of the crown position percentage is 65.1005642% (0% means that position is at the root of the tree and 100% means position is at the top of the tree), for the percentage value equal 0 means that there is no crown in this tree, which mean it might only be a trunk and there is no tree's



Figure 4. The location percentage of each tree crown of 559, the red line is the mean value of crown position.

crown area is locating at the top (Figure 4).

The second part is merge all the upper crown points, roots points (Figure5, B) as well as local DEM together.

The last part of is generating the ALS model through canopy-ground point cloud (Figure5, D). The ALS model (convert by TLS) displays in the Figure 5 (E, Ea). Compared the ALS model (convert by TLS) with ALS by using cloud to cloud distance in CloudCompare (Figure 6), it illustrates that ALS model (convert by TLS) perfect fit with the ALS point cloud, about 95% of the distance between ALS model (convert by ALS) and ALS are under the 3.163323 m. the ALS model (convert by TLS) canopy area which the color is blue presents the simulate ALS model is fine, which distance

gap is less than 0.530873m. Compared the ALS model (converted by TLS) with TLS with the same method as previous, this ALS model shows more match with TLS, as about 95% of the distances between ALS model and TLS point cloud are under 1.56743m. the canopy area which the color is blue presents the simulate ALS model have less error compared with the initial TLS point cloud, which the cloud to cloud absolute distances are less than 0.307324m(Figure 7).

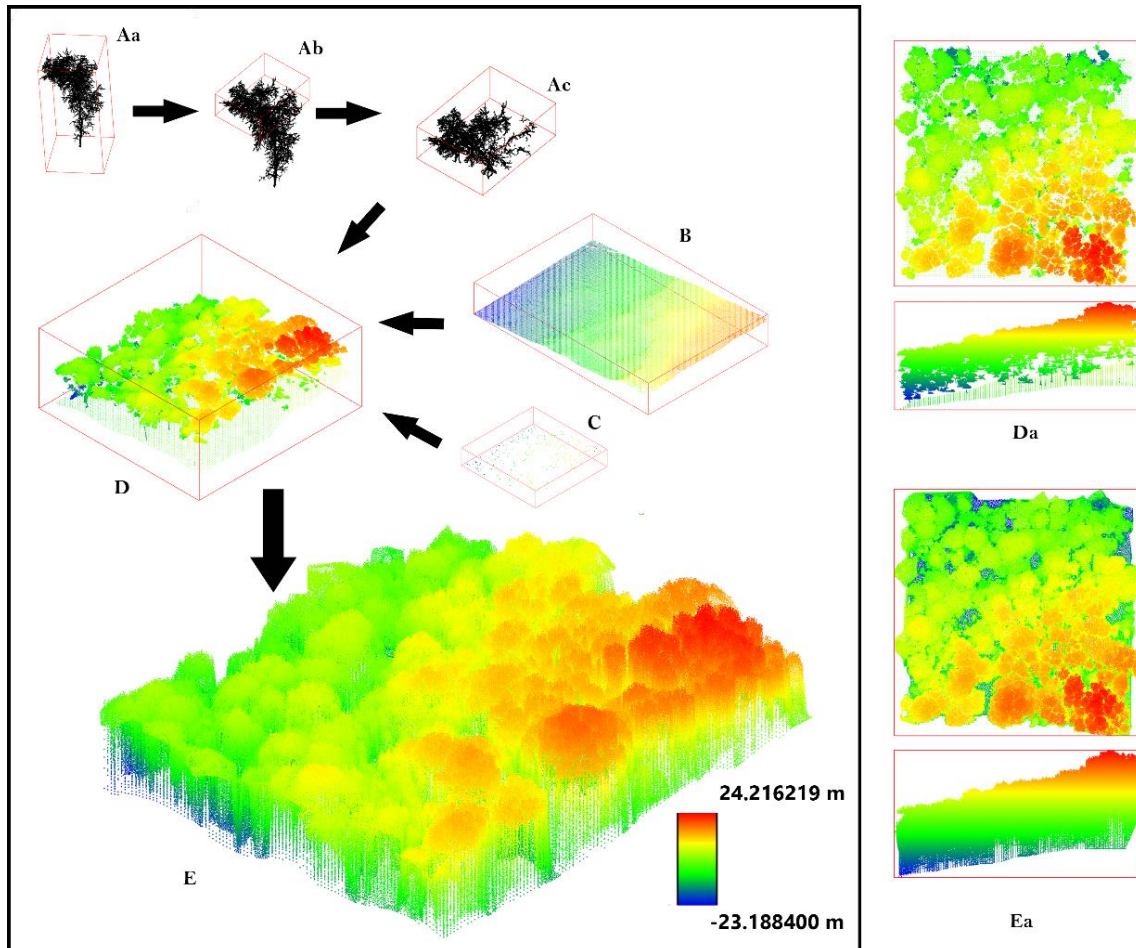


Figure 5. Visual flow chart of generating the ALS model from individual TLS tree point cloud. Aa is an individual TLS tree point cloud; Ab is selecting the canopy from individual TLS tree; Ac is canopy area; B is the local DEM of study site; C is all 559 root points extracted from TLS trees; D is the initial canopy-ground point cloud merged by A, B and C, Da is the top and side views of canopy-ground point cloud; E is the ALS model converted by D, Ea is the top and side views of ALS model.

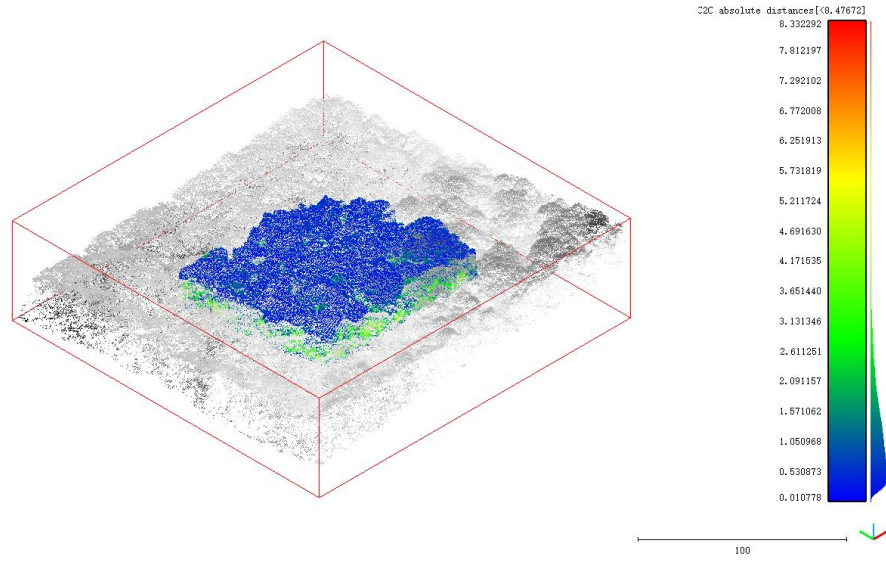


Figure 6. Cloud compared result between ALS model and ALS, the color illustrates the cloud to cloud absolute distance.

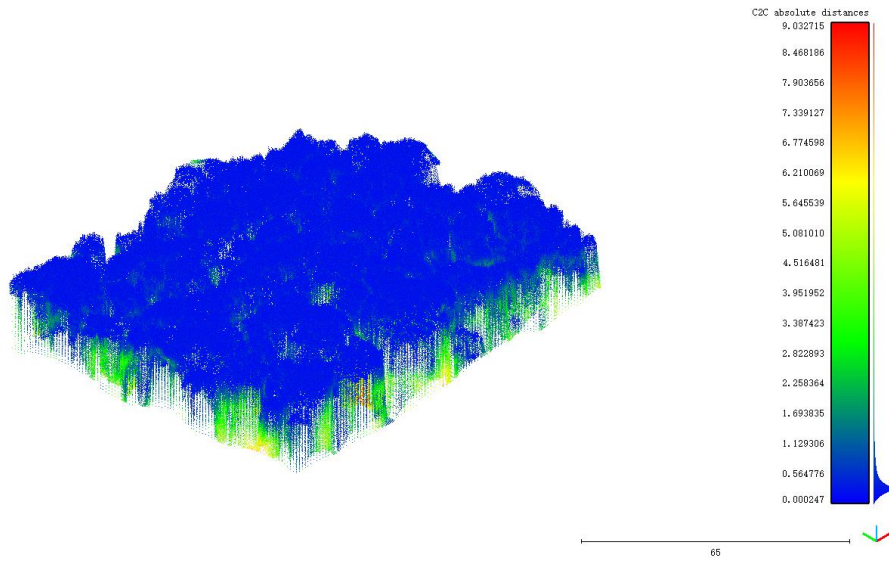


Figure 7. Cloud compared result between ALS model and TLS point cloud, the color illustrates the cloud to cloud absolute distance.

4.2 Ground and vegetation area extraction

By applying the Cloth Simulation Filter (CSF) in CloudCompare, the ground point cloud and the off-ground point cloud (vegetation) are extracted by ALS model (convert by

TLS). According to the cloud to cloud distance calculation, the result displays the distance gap between ground and local DEM in Figure 8. From the result, it presents that the ground area fit fine with the local DEM, which about 95.202% points' distance distribute under 3.362801m. The blue area shows the ground point is perfectly match the ground point with DEM, which are less than 0.493511m.

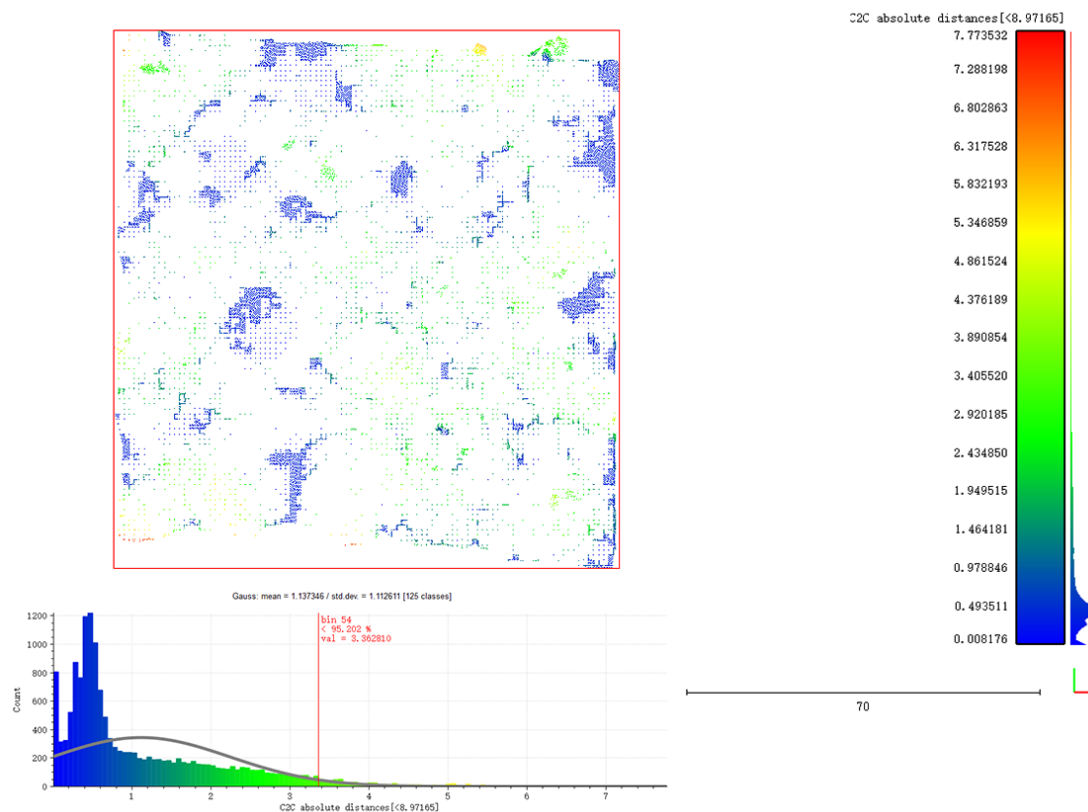


Figure 8. Cloud compared result between ground point from ALS model and DEM point cloud, the color illustrates the cloud to cloud absolute distance.

4.3 From crown perimeter (CP) to diameter at the breast height (DBH)

To gain the relatively accurate linear regression between crown perimeter (CP) and diameter at breast (DBH), it is necessary to calculate from the 559 trees of the study area. If all the tree was used to generate one linear regression equation (Figure 9A; $DBH = 1.81 \cdot CP - 11.33$), there are negative value in DBH when CP less than 6.25m. hence, to prohibit this kind of circumstance, the CP was divided into 2 parts to generate the linear regression. When $CP < 10m$, the linear regression present in Figure 9B ($DBH = 0.43 \cdot CP + 2.48$), When $CP \geq 10m$, the linear regression present in Figure 9C

($DBH = 2.04 \cdot CP - 17.25$).

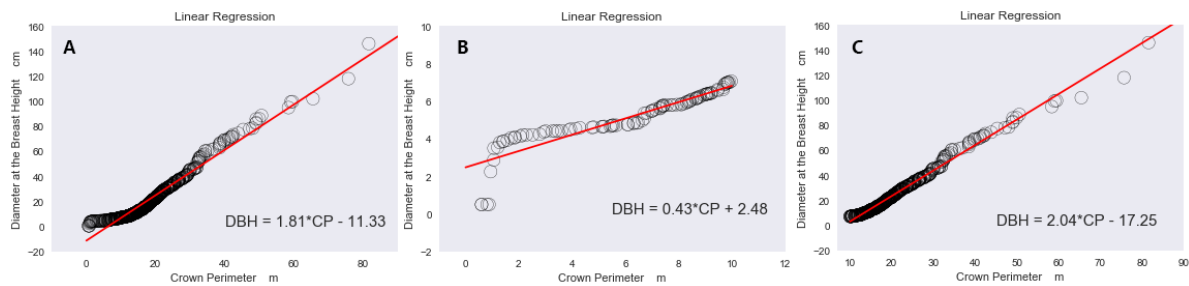


Figure 9. Linear Regression of CP and DBH, which statistics from 559 TLS point cloud trees and LeafData_3Dmodel_metadata.xlsx

4.4 Tree segmentation

Tree segmentation code is supported by Hamraz (2016), as previous mention in 3.4.2, there is one parameter can noteworthy influence tree delineation result, which is the `NOMINAL_POST_SPACING`. The default value of it is 0.85, the correspondent Tree segmentation result is 60 (Figure feffeefef). In this project, it also applies the `NOMINAL_POST_SPACING = 0.5` and `0.3`. The result of estimating the AGB is utilizing when `NOMINAL_POST_SPACING` equals 0.3 and the reason why using `NOMINAL_POST_SPACING = 0.3` and how it present will be explain in next section (Figure hadkkff). The `MINIMUM_DETECTABEL_CROWN_WIDTH` changes over `NOMINAL_POST_SPACING`, which normally 4 times as `NOMINAL_POST_SPACING`. Another adjusted required parameter is `MINIMUM_TREE_HEIGHT`, which is set as 2 (All the parameters unit in the code are feet) in this project. According to code statistics, there are 456999 return points are loading into the tree segmentation code, 110 trees are segmentation when the `NOMINAL_POST_SPACING` equals 0.5 while 219 trees are detected when the `NOMINAL_POST_SPACING` equals 0.3. The segmentation result will present through point cloud (3D) as well as the boundary point in a csv file instead of 2D raster, which means the result can be regarded as the ALS point cloud are divided into 219 individual point cloud. Each point cloud can be regarded as a tree, consequently, each tree point cloud can find the height, CP and tree top easily.

4.5 Tree species geo-referencing

As mentioned in methodology, after gaining the tree tops from each individual tree segmentation point cloud, those top points were linked with tree species. Figure 10 provided the position of 219 ALS tree tops and TLS trees corresponded with ALS 219 trees as well as all 559 TLS' s position with species. In this way, it registers all the ALS trees with TLS trees.

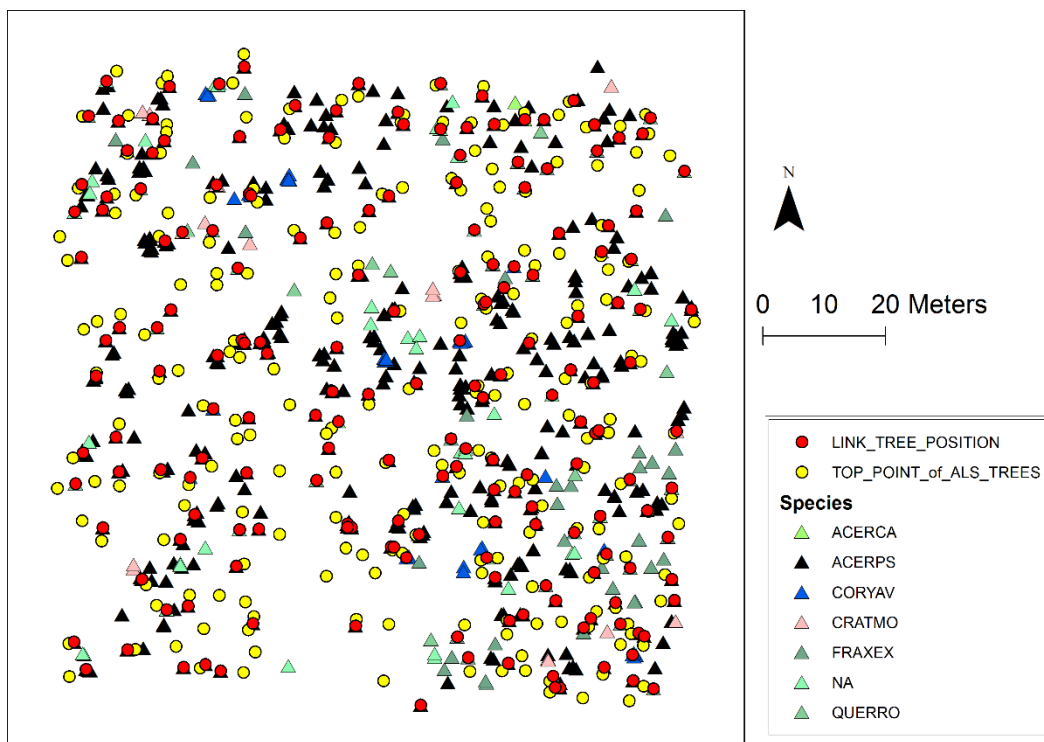


Figure 10. The position of all ALS tree tops and TLS trees corresponded with ALS trees as well as all 559 TLS' s position with species

After registration between ALS trees and TLS trees, the new statistic result shows that there are 164 Sycamore (*Acer pseudoplatanus*), Taxonomic code as ACERPS; 1 Field maple (*Acer campetre*), Taxonomic code as ACERCA; 9 Common hazel (*Corylus avellana*), Taxonomic code as CORYAV; 4 Common hawthorns (*Crataegus monogyna*), Taxonomic code as CRATMO; 21 European ash (*Fraxinus excelsior*), Taxonomic code as FRAXEX, 14 Pedunculate oak (*Quercus robur*), Taxonomic code

as QUERRO; as well as 6 unknown species trees.

4.6 AGB estimation

In this project, the AGB was estimated through species-specific allometric equation, plot area allometric equation as well as volumetric equation.

4.6.1 Species-specific allometric equation

Estimating the AGB by applying species-specific allometric equation require all the detected ALS trees correspondence to the TLS tree in species. This project statistics from all the TLS trees by applying the species-specific allometric equations which mentioned previously, however, due to there are 41 unknown species, it cannot be applied in any allometric equation. These unknown trees are not counted into estimating the AGB. From the Table 3, it illustrates that the AGB of 388 Sycamore (2 Field Maples included) is 180.9602 t, the AGB of 52 European Ash is 36.92901t, 24 Oaks' AGB weight 91.04594t. And 54 Hawthorn weights 456.1874(35 hazel included). The overall AGB of the known species in the 1-hectare study site weights 765.1226t. The correspondence of the ALS detected tree results show in Table 4: 165 Sycamore weight 162.4803t, 21 European Oak's AGB is 23.16084t, 14 Oak weight 9.651312t and Hawthorn's AGB weights 1008.825t and the overall AGB estimated by species-specific allometric equation is 1204.118t. Total AGB estimated by ALS is much larger than TLS, which means the method applied in study site is overestimated. Apparently, Hawthorn's AGB takes up a sizeable proportion of overall AGB in this method both in TLS trees (83.7819%) and ALS trees (59.6228%). Considering of the number as well as the proportional weight of the Hawthorn, it is a worth debate result which will be discussed later. To reduce the effect of Hawthorn, this project also calculates the AGB excluded the Hawthorn, it only statistics Sycamore, European Ash, as well as Oak and calculate the above 3 species' AGB both in all TLS dataset (308.9351518 t) and ALS dataset (195.2924275t). For Sycamore, European Ash as well as Oak, estimated ALS AGB can take up 63.215% of estimated TLS value.

Table 3. AGB estimation from species-specific allometric equation derive from TLS tree point clouds

Number	Species	AGB (t)	Equation	Average AGB (t)
386	Sycamore	155.46498	2	
	Sycamore	206.45542	3	180.9602021
52	European Ash	32.544682	4	
	European Ash	41.313342	5	36.92901202
24	Oak	68.434589	6	
	Oak	57.286225	7	
	Oak	144.99547	8	
	Oak	93.467471	9	91.04593769
54	Hawthorn	456.18742	10	456.1874215
Total number of the tree:				517
Sum of the AGB (t)				765.1225732
Proportion of the Hawthorn weighs				0.596227895
Sum of the AGB excluded Hawthorn (t)				308.9351518

Table 4. AGB estimation from species-specific allometric equation derive from ALS model

Number	Species	AGB (t)	Equation	Average AGB (t)
164	Sycamore	138.81763	2	
	Sycamore	186.14292	3	162.4802737
	European Ash	20.617006	4	
21	European Ash	25.704678	5	23.16084187
	Oak	7.8046943	6	
	Oak	6.7141192	7	
	Oak	14.3884	8	
14	Oak	9.6980342	9	9.651311954
13	Hawthorn	1008.8253	10	1008.82534
Total number of the tree:				213
Sum of the AGB (t)				1204.117768
Proportion of the Hawthorn weighs				0.837812851
Sum of the AGB excluded Hawthorn (t)				195.2924275

4.6.2 Plot area allometric equation

Plot area allometric equations are applied in large scale area to estimate the AGB, it also applied in this study site. It does not need all species' allometric equations, for the study area, All the tree species can be divided into 3 parts: for all the Sycamores and Field Maple as beech, for common Hazel, Hawthorn, European Ash as Oak as Oak and for the unidentified trees as Na. The Beech and Oak's allometric equations have already been mention previously, and the AGB can be calculated based on different DBH. For unidentified trees, they calculate the biomass also based on Beech and Oak's allometric equation, according the Beech's proportional coefficient with Oak's, the unidentified trees are divided into Beech and Oak to estimate the AGB (Equation 11). **Table 5** illustrates that the AGB of all TLS tree point cloud calculated by plot area allometric equation is 51.54631739t and as for ALS tree point cloud, the sum value of AGB is 36.25972493t (Table 6). Compared the plot area allometric equation result with species-specific allometric equation result, the plot area AGB value from the TLS is approximately tenth of value which calculated by species-specific equation. The ALS estimated AGB takes up 70.344% of the TLS estimated AGB. Plot area allometric equation is better than species-specific equation from the view which is more closed to the TLS estimated AGB separately. Equation 11 illustrates that how to calculate the unidentified tree' s AGB.

$$AGB_{NA} = \frac{Beech}{Beech + Oak} AGB_{NA(Beech)} + \frac{Oak}{Beech + Oak} AGB_{NA(Oak)} \quad (11)$$

Table 5. AGB estimation from plot area allometric equation derive from TLS tree point cloud model

Total number of each species	Species	number of trees	DBH range (cm)	AGB t
388	Beech	51	DBH<7	0.163402
		310	7=< DBH<=50	17.27469
		27	DBH>50	16.40512
130	Oak	25	DBH<7	0.08138
		83	7=< DBH<=50	3.180807
		22	DBH>50	12.78476
41	Na	22	DBH<7	0.070917

	19	7=< DBH<=50	1.585247
	0	DBH>50	0
Total tree number			559
Total AGB (t)			51.54631739

Table 6. AGB estimation from plot area allometric equation derive from ALS model

Total number of each species	Species	number of trees	DBH range (cm)	AGB t
165	Beech	34	DBH<7	0.133808
		97	7=< DBH<=50	8.253235
		34	DBH>50	20.82566
48	Oak	9	DBH<7	0.026168
		29	7=< DBH<=50	2.11784
		10	DBH>50	3.758364
6	Na	2	DBH<7	0.00585
		2	7=< DBH<=50	0.291329
		2	DBH>50	0.847475
Total tree number				219
Total AGB (t)				36.25972493

4.6.3 Volumetric equation

Volumetric equation is the only method involved the Height of the tree. In this project and the height is calculated by finding vertical height of each segmentation tree point cloud, which will increase more bias for estimating the AGB. Because of the previous research(Brodmeado et al, 2005) only offering the Volumetric equation for Sycamore, European Ash as well as Oak in UK. For the rest of the species existing in the study area, according to the volume statistics from TLS file, the Hawthorn, Hazel and Field maple as well as unidentified trees only take up a small proportion compared with the whole volume of the study site, about 1.4572% (Table 7). Hence, the volume of those species can be ignored, or those trees can be regarded as Sycamore to be estimated and the wood density of unidentified trees can be regarded as density of Sycamore as well. Table 8 illustrates that total volume as well as volume only included Sycamore, European Ash and Oak which are 247.2410454 m³ and 237.882663 m³ and the total

AGB value of the estimating ALS tree is 158327.6 kg, which takes up 32.90% of the TLS AGB. Theoretically, the calculated height should be the same as TLS statistics as the xlsx file provided. However, according to Linear Regression generated by TLS tree height(H_{re}) and ALS tree height (H_{ca}), as the Figure 11 Illustrates, the Linear Regression equation is $H_{ca} = 0.1 \cdot H_{re} + 10.76$, which means for most of Heights which were calculated by ALS are underestimated. Take 1m Tolerance Value, there are about 155 of 219 height being underestimating which take up 70.708% of all the trees. Those underestimated trees' heights are centralized on the range over 13.07m. Although there are 24.210% of the heights being overestimated, the range of those tree are located at the value less than 10.84 m. Therefore, when those height go into the volumetric equation, they might cause the value of AGB less than the theoretical value.

Table 7. AGB estimation from volumetric allometric equation derive from TLS tree point cloud

43	Na	615	2.9139	1792.049
386	Sycamore	615	516.70075	317771
19	Hawthorn	850	3.00976	2558.296
52	European Ash	680	96.43252	65574.11
24	Oak	675	133.814	90324.45
35	Hazel	627	5.12153	3211.199
Sum of AGB excluded Na (kg)				479439
Sum of AGB (kg)				481231.1
Number of trees				559
Total volume (m³)				757.99246
Volume of Sycamore, European Ash and Oak(m³)				746.94727

Table 8. AGB estimation from volumetric equation derive from ALS model

Number of each species	Species	Wood density (kg/m³)	Volume (m³)	AGB (kg)
7	Na	615	5.391107059	3315.531
164	Sycamore	615	139.5024989	85794.04
4	Hawthorn	850	0.998525748	848.7469

	21	European Ash	680	20.25228129	13771.55
	14	Oak	675	78.12788282	52736.32
	9	Hazel	627	2.96874958	1861.406
Sum of AGB excluded Na		(kg)			155012.1
Sum of AGB (kg)					158327.6
Number of trees					219
Total volume (m³)					247.2410454
Volume of Sycamore, European Ash and Oak(m³)					237.882663

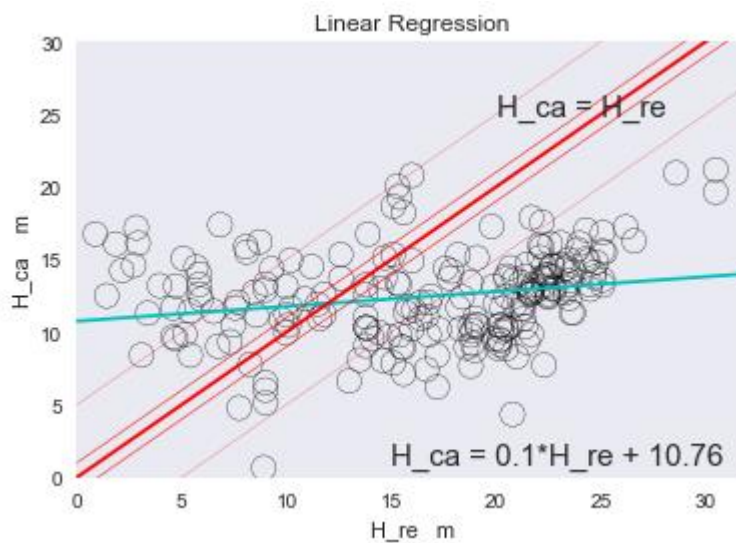


Figure 11. Linear Regression between TLS tree height(H_{re}) and ALS tree height (H_{ca}) (blue) as well as the relationship between TLS tree height and ALS tree height in theoretical and threshold of 1m and 5m (red).

5. Discussion

In this section, it will divide into 6 parts to discuss about estimated results of AGB and the effects or the bias to the results which brought by processing procedure and each method.

5.1 Discussion about ALS model

In this project, the material of applying to estimate the AGB is ALS model which convert by TLS. As previous mentioned in section 4, to the validate the accuracy of the ALS model (convert by TLS), the model is used to compared with ALS point cloud. From the cloud compared result (Figure 6), it illustrates the upper canopy area is perfect

match with the ALS point cloud. The distance from ALS model (convert by TLS) to ALS point cloud are less than 0.5m, which fall within the acceptable range. For point cloud of ALS (convert by TLS) located in the middle area, below the canopy, the error increase. However, the point cloud in this part almost does not influence the tree segmentation result. The boundary point cloud of simulate ALS model should be processed carefully, since it might increase the invalid tree segments thus affect the AGB. There is one thing needed to be discussed is that the upper canopy area selected might cause the crown area shrink. We applied the method to select upper crown area is by finding the maximum distance both x direction and y direction in vertical range of individual tree and choose the largest distance's location in either x direction or in y direction. It can choose the crown area for individual tree efficiently in some extent, however, for a cross-section of a tree, it is a 2D polygon. The maximum distance for a 2D polygon might not always be in x direction or y direction. For the trees' maximum distances are not in x or y direction as well as this area's location is below the location of maximum distance from x and y, the selected crown position will be different from real crown position and the selected crown area will be smaller than the real crown area, which might cause the estimated AGB decreased for individual tree. The shrink crown for individual tree makes the gap among different tree increase, which raise the likelihood of segmenting more trees from the ALS model (converted by TLS).

5.2 Discussion on the crown perimeter (CP) to DBH

For most research (Dalponte, M., et al, 2018; Chukwu, O., Dau, J.H. and Ezenwenyi, J.U., 2017), crown diameter (CD) was regard as an important parameter to generate the DBH. However, the crown diameter is hard to be defined and it can be calculated varies based on different methods, such as cross-method, average crown spread as well as Spoke method, which might bring different kind of bias according to different method. Hence, in this project, it skips finding a relative uncertainty CD value, instead, by calculating a relative uncomplicated CP from calculating the boundary length of the polygon. According to statistics all the 559 TLS trees' CP and DBH, this project generates a linear relation between DBH and CP, the result was illustration in section 4.3. For the $CP < 10$ m, the mean squared error of the linear regression is 0.6 and the variance score is 0.69, which means it is a relatively good linear regression model. For the $CP \geq 10$ m, the mean squared error is relative large which is 4430.99 and the

variance score is negative, which means it is not a good linear model (Figure 9).

5.3 Discussion on tree species geo-referencing

Before applying allometric or volumetric equation to estimate the AGB, it is necessary to link the species (TLS) layout with segmentation trees. Near analysis can help with linking the ALS tree with TLS tree. The simple explanation is selecting 219 trees from 559 trees of known species. However, this algorithm can only find the nearest ALS tree's position with the reference TLS point. To register a ALS tree with right TLS tree, except for considering if the point of TLS tree's position is the nearest point to the ALS tree top, the height of tree need to be considered as well. For tree segmentation algorithm, it delineates the first tree from the overhead Angle. For high density woodland, there are always higher tree overlap the lower trees which are preferential selection due to its location is closer than the taller tree. Hence, the Near analysis will register a smaller tree or varied species TLS tree with ALS tree, which might influence the AGB estimation eventually by applying different allometric equation and volumetric equation, especially for the species-specific allometric equation, because the AGB is sensitive to the species, growth as well as allometry (Evans et al., 2015). To solve this bias, Yu et al. (2017) developed a solution by using multispectral ALS data, they extracted tree feature according to point cloud features, single channel intensity features as well as other features as predictors and build prediction models. According to the research, single channel intensity feature can reach 85.9% of the correction, which is the most accurate tree species classification of multispectral ALS data.

5.4 Discussion on tree segmentation results

Figure 12 displays the all individual TLS tree crown polygons' layout. Apparently, there are overlapping area like the south east corner of the study area, hence, there will be trees cannot be seen from the top view angle. When converting the TLS to ALS, all the overlapping tree point cloud will be merged together. What's more, there will be the circumstance that a ground of trees with similar heights growing together, their canopies are intersected. Also, for some large trees, they might have different branches. All these circumstance increases the bias of tree segmentation. To segment as many as valid individual tree point cloud from the ALS (converted by TLS), suitable parameters should be set. Figure 13,14 and 15 display that the smaller NOMINAL_POST_SPACING value as well as corresponding parameter changed, the more tree will be delineated from the ALS model. For the high-density woodland

delineation, the hardest part is to separate the huddled trees. A larger NOMINAL_POST_SPACING will cause the several trees are recognized into one piece of segmentation area as the figure shows. However, when the parameter values are small to a certain extent, there will be the circumstance that the large tree are segmented into different small trees, as the Figure 15 display. Hence, considering the above conditions, 0.3 was chosen as the NOMINAL_POST_SPACING for estimating the AGB in this project. Although the largest tree was divided into 2 trees, there are more smaller trees being recognized, which will increase the accuracy of estimating the AGB.

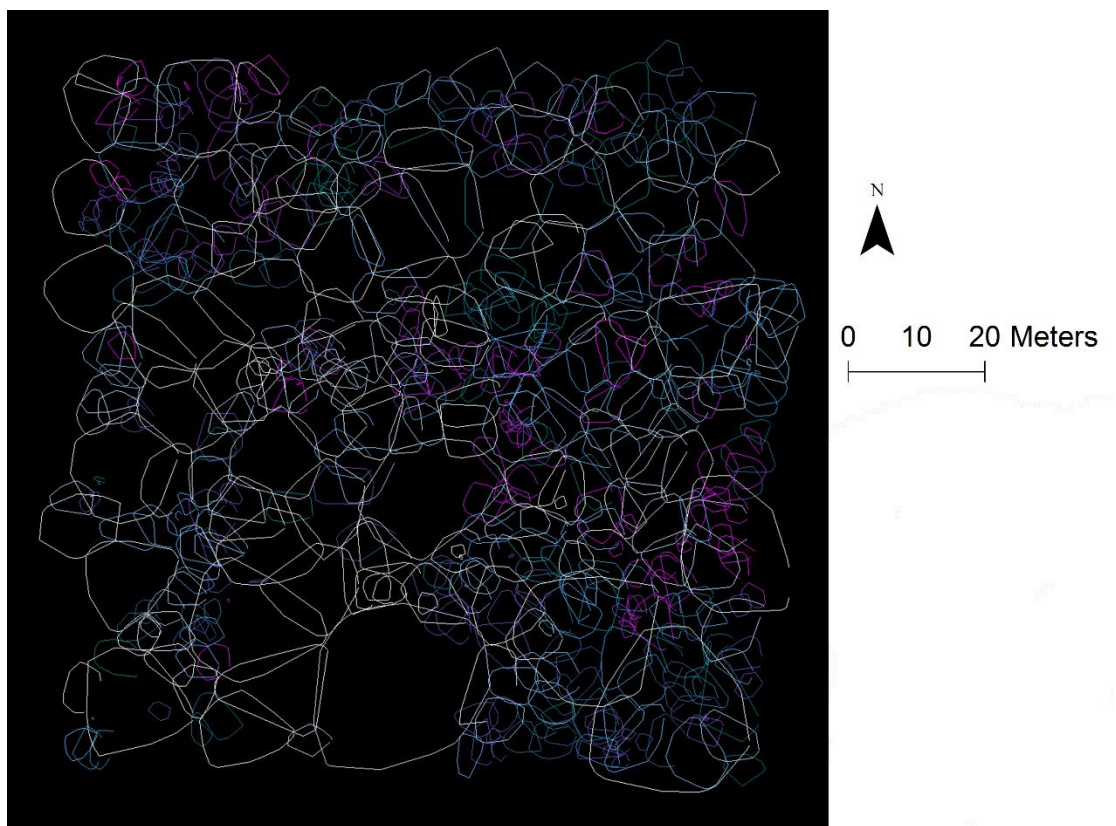


Figure 12. the layout of 559 TLS trees' crowns in the top view, which generated by OpenCV in python(Appendix A)

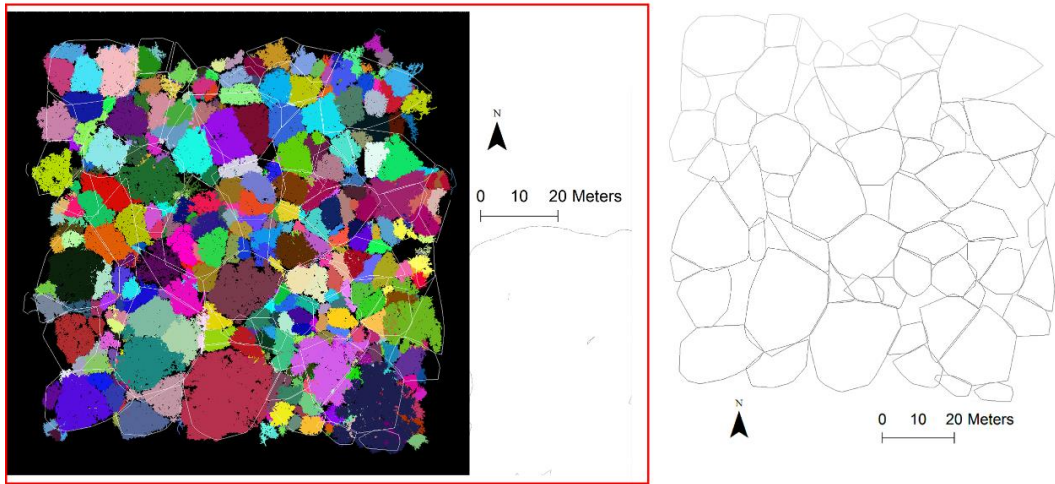


Figure 13. tree segmentation result derives from ALS model (NOMINAL_POST_SPACING = 0.85)

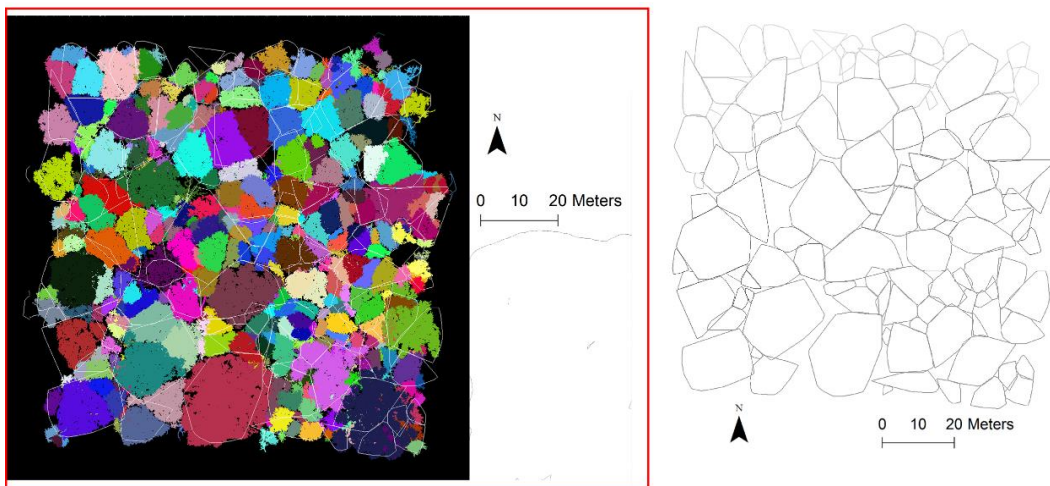


Figure 14. tree segmentation result derives from ALS model (NOMINAL_POST_SPACING = 0.5)

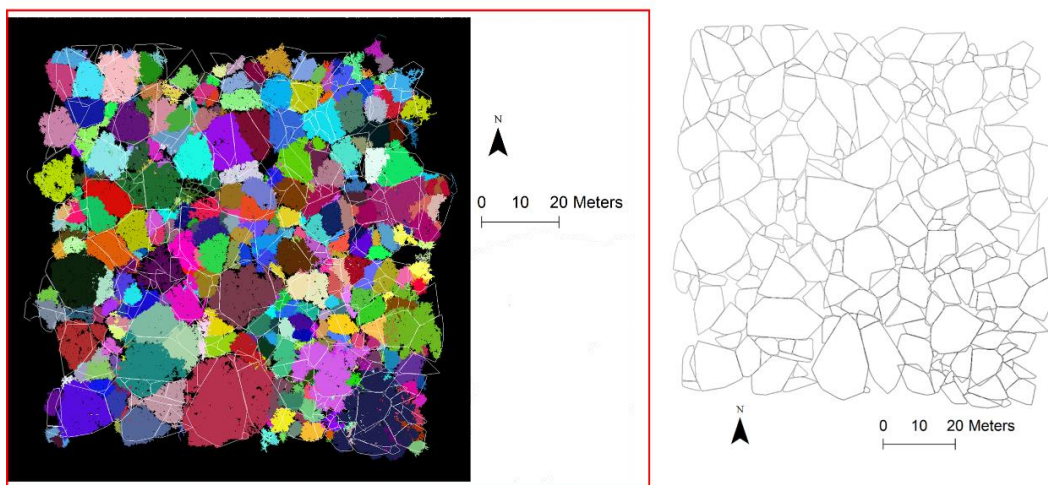


Figure 15. tree segmentation result derives from ALS model (NOMINAL_POST_SPACING = 0.3)

5.5 Discussion on results of estimated AGB

Theoretically, to evaluate the results of estimated AGB from different methods (the above three mentioned in section 3.4.4 and 3.4.5). The best reference data to validate the results of estimated AGB is via destructive measurement, however, it is impractical to operate. Hence, in this project, it utilizes the TLS parameters which are calculated by QSM algorithm (volume, height, DBH) to calculate the AGB based on different allometric or volumetric equation to compare with ALS AGBs which are calculated according to different allometric or volumetric equation correspond to the TLS's AGB.

5.5.1 Discussion on species-specific allometric equation.

Apparently, the Hawthorn allometric equation is obviously an invalid method for calculating the AGB in the study site, since the 19 common hawthorns and 35 common hazel's AGB which apply hawthorns allometric equation to be calculated in 559 trees take up 59.6% of total AGB for TLS trees. It can be caused by the applied inappropriate allometric equation. Compared with sum of ALS AGB with the sum of TLS AGB, the ALS AGB is overestimated. The reason might cause the overestimate which is due to the inaccuracy of geo-referencing of the ALS trees with TLS trees. To get rid of the influence from hawthorn, only Sycamore European Ash and Oak are collected to recalculate the AGB and evaluate the results. After recalculating and comparing the new ALS AGB with TLS AGB. There are 63.215% AGB can be estimated from the study site. This method is highly influenced by species and DBH, with a higher accuracy in DBH and species, the result might be more accurate.

5.5.2 Discussion on plot area allometric equation

The AGB which is estimated by plot area allometric equation seems to take quite a minor part compared with other methods, might be a tenth of other methods. However, it can estimate 70.344% of the whole plot area, the result is closer to TLS estimation compared with species-specific allometric equation. However, this method is also influenced by inaccuracy of geo-referencing. As there is no tree's DBH over 50cm of the unidentified tree of TLS trees and it has 2 trees' DBH over 50cm in ALS trees (Table 5 and Table 6). With less impact of species on the method, the DBH becomes the main influencing factor to AGB estimation. However, the AGB value estimated by plot area allometric equation differs from other two methods in order of magnitude as the Figure

15 displays.

5.5.3 Discussion on volumetric equation

The result of volumetric equation takes up 32.90% of total AGB, which is least realistic approach of three methods (Table 3, 4, 5, 6, 7 and 8). Just like the previous analysis in section 4.6.3. the height presence increased of the bias for estimating the biomass. Indeed, this method is also influenced by the inaccuracy of geo-referencing. Due to the bias of DBH, Height and Species as well as the result of the AGB, this method seems to be the worst method to estimate the AGB of three methods in this project.

5.6 Discussion the limitation and implication

Above three methods of estimating AGB all have the relationship with DBH. For the allometric equations using in this project, they are only influenced by DBH. As for the volumetric equation, they were contributed by DBH as well as Height. Hence, the DBH is a significant important parameter which contribute to estimating the AGB. In this project, Crown perimeter is used to estimate DBH, which makes the transfer equation from CP to DBH important in estimating AGB. To validate the linear regression between CP and DBH, two aspects can be regarded as reference: The first one is through the variance score, as mentioned previously in section 5.2. when DBH less than 10m, it is a relative fine linear model, however when DBH over as well as equal 10m, it is not a good model of two parameters, which will increase the uncertainty of AGB estimation. Another reference is through compared the ALS AGB with TLS AGB. However, before the comparison, it is necessary to rescale the ALS AGB to decrease the influence from the state of growth of high-density forest in the study site, for example, the higher trees overlap the shorter trees, a tree has many branches as well as the canopies intersect. From Table 9, it displays the rescale AGB of three methods. According to the previous discussion of three estimating methods, the AGB calculated by plot area allometric equations is used to verify linear regression due to it is less effect by species and other factor except for the DBH. As the result (Table 9, (1)) illustrates, the scale of AGB is 92.50151t, which is larger than the TLS estimation. Hence, the result illustrates the linear regression of DBH and CP might make the AGB overestimated. Calculating the DBH by using Crown perimeter is used in this project which provides great uncertainty for calculating the AGB due to it has been applied few in other studies. If we want to improve the accurate of the result, it is better to gather more statistics data of CP and DBH. Alternatively, using the relationship

between Crown diameter and DBH might help.

Table 9. Rescale AGB from three methods: (1) AGB derives from species-specific allometric equation. (2) AGB derives from plot area allometric equation. (3) AGB derives from volumetric equation.

						Rescale AGB t
						(1)
Sycamore						
382.4230832						456.318845
European Ash						1
57.3506556						1
Oak						1
16.5451						1
Beech						(2)
68.69411372						92.5015068
Oak						9
15.9855908						3
Na						2
7.82180						2
Hazel						(3)
Na	Sycamore	Hawthorn	European Ash	Oak	Hazel	
20.3668	201.9299	4.031548	34.10098095	90.40512	7.23880	358.073157
3					1	8

In this project, using ALS point cloud which converted by TLS can decrease the gap between the ALS and TLS, especially for the boundary area. It can solve the issue that the ALS point cloud cannot perfectly match the TLS and reduce the bias brought by primary data. As the cloud compared result between the ALS (converted by TLS) and TLS (), it illustrates that the ALS model (converted by TLS) is perfect fit with the TLS, about 95% of the point distance less than 2.5m. For the canopy area, the ALS and TLS are matched perfectly. But for the ground area, the result is not as perfect as canopy, which might influence the height extraction and that affects the volumetric equation and has no influence in allometric equation due to the only parameter is DBH. Hence, the ALS (converted by TLS) can increase accurate of AGB estimation for allometric equation. The model of generating ALS model might bring the bias for estimating the AGB since the inaccurate crown area selected as section 5.1 has been discussed. Broadly speaking, this simulated ALS model has strong potential for allometric equation validation and calibration as well as the future study in estimating AGB.

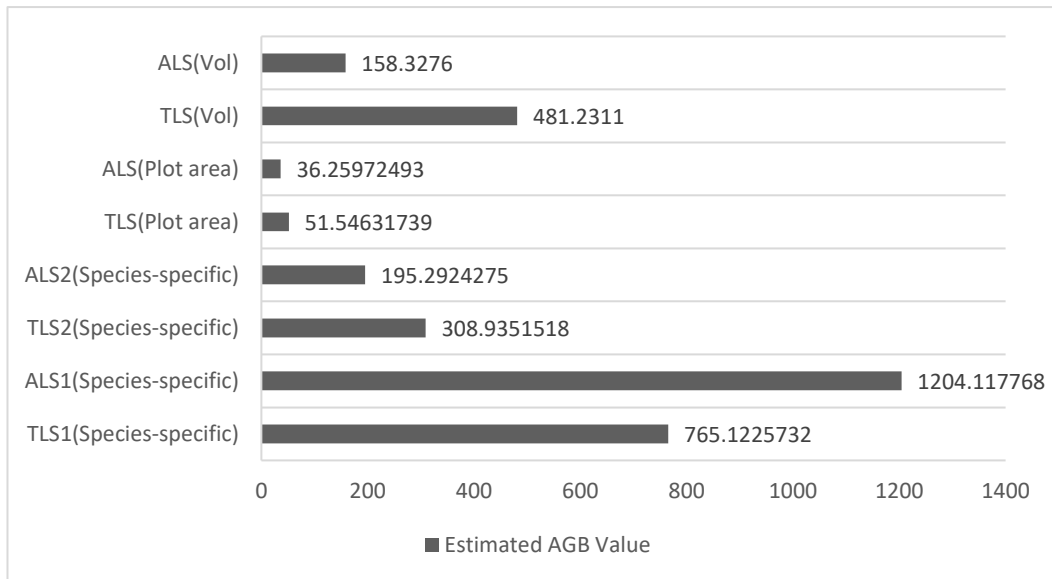


Figure 16. Bar chart of total AGB estimation from different allometric and volumetric equations; ALS1/TLS1 represent all species without unidentified trees and ALS2/TLS2 represent all species without Hawthorn and unidentified trees

6. Conclusion

Calculating the AGB by combining active remote sensing with allometric equation has been widely used to comprehend carbon storage in the terrestrial ecosystems. ALS regarded as a relatively accurate and easy to obtain data become a popular active remote sensing data source for AGB estimation. However, using ALS point cloud with allometric or volumetric equations to generate the AGB has a large bias with the actual value and need to be validated as well as calibrated for further study.

In general, as the destructive method cannot be applied to validate the method, TLS estimation replaced the destructive method as the reference. To decrease this bias, in this project, a ALS model was converted by TLS is applied to decreased bias brought by the ALS point cloud, like the ALS point cloud cannot perfectly match the TLS point cloud especially in the boundary area. The ALS model build in this project, perfect match resource TLS point cloud according compared the ALS point cloud and TLS point cloud.

Basing on the relatively accurate ALS model, this project also tests three kinds of methods for AGB estimation (species-specific and plot area allometric equation as well as volumetric equation). Evaluating the uncertainty and bias of each equation and

discussing the uncertainty and bias from the ALS model and process of calculating the AGB. From the result and discussion, the bias and uncertainty factors are from the growth characteristic of high density woodland, the crown selection in TLS, CP to DBH, tree segmentation parameters, species link from ALS to TLS, DBH for allometric equation as well as height and DBH for volumetric equation. According to comparing three methods of estimating the AGB (Figure 16), species-specific allometric equation is the most valid method to estimating the AGB regardless of the Hawthorn which takes up 63.215% of the reality AGB because the AGB calculated by plot area allometric equation is not satisfied comparing with the other two methods and the ALS AGB calculated by volumetric equation are two low comparing with TLS AGB.

Finally, to gain a relative accurate AGB by using the method in this project, the method of generating DBH and species geo-referencing are highly recommended to be improved in the future work.

7. Auto-Critique

The original topic is “Combining terrestrial and airborne LiDAR data for estimating biomass and allometry for woodland trees in the UK”. It simply applies the tree segmentation code to delineate the trees on the ALS data and estimates the AGB, then, uses the AGB derived from TLS data to validate the AGB derived from ALS. However, the ALS point cloud’s area is much larger than TLS point cloud when applying the AGB estimation comparing. Cutting the ALS point cloud into TLS size might be one option to make the validation more accurate, however, it still has the bias that the ALS point cloud cannot register with TLS point cloud perfectly. What ‘s more, the boundary area might exist residual in the ALS point cloud might be increase the AGB estimation. Hence, it is necessary to find a way to generate an accurate ALS point cloud so that it can be validated with the known TLS data and analyse. The reason why choosing this topic is due to my interest in ALS and TLS point cloud processing and programming.

Hence, this project generates a ALS model by using TLS point cloud to recalculate the ALS AGB compared with previous work. however, when I try to calculate the DBH. The applying resource and method is not good as I suppose which need to be improved in the future work. But for the ALS model, it represents quite good compared with ALS and TLS point cloud

8. References

- Åkerblom, M., Raunonen, P., Mäkipää, R. and Kaasalainen, M., 2017. Automatic tree species recognition with quantitative structure models. *Remote Sensing of Environment*, 191, pp.1-12.
- Anaya, J. A., Chuvieco, E., & Palacios-Orueta, A. 2009. Aboveground biomass assessment in Colombia: A remote sensing approach. *Forest Ecology and Management*, 257(4), 1237-1246.
- Anaya, J.A., Chuvieco, E. and Palacios-Orueta, A., 2009. Aboveground biomass assessment in Colombia: A remote sensing approach. *Forest Ecology and Management*, 257(4), pp.1237-1246.
- Araújo, T. M., Higuchi, N., & de Carvalho Júnior, J. A., 1999. Comparison of formulae for biomass content determination in a tropical rain forest site in the state of Pará, Brazil. *Forest ecology and management*, 117(1), 43-52.
- Austin, J. M., Mackey, B. G. and van Niel, K. P., 2003. Estimating forest biomass using satellite radar: an exploratory study in a temperate Australian Eucalyptus forest.. *Forest Ecology and Management*, 176: pp. 575–583.
- Barbosa, P. M., Stroppiana, D. and Gregoire, J. 1999. An assessment of vegetation fire in Africa 1981–1991: burned areas, burned biomass, and atmospheric emissions.. *Global Biogeochemical Cycles*, 13: pp. 933–950.
- Broadmeadow, M. S. J., Matthews, R. W., Mackie, E., Wilkinson, M., Benham, S., & Harris, K. (2005). 6. Survey Methods for Kyoto Protocol Monitoring and Verification of UK Forest Carbon Stocks. *UK Emissions by Sources and Removals by Sinks due to Land Use, Land Use Change and Forestry Activities*, 6, 2.
- Brown, S., 1997. Estimating biomass and biomass change of tropical forests: a primer (Vol. 134). Food & Agriculture Org.
- Brown, S., Gillespie, A. J., & Lugo, A. E., 1989. Biomass estimation methods for tropical forests with applications to forest inventory data. *Forest science*, 35(4), 881-902.
- Bunce, R. G. H., 1968. Biomass and production of trees in a mixed deciduous

woodland: I. Girth and height as parameters for the estimation of tree dry weight. *The Journal of Ecology*, 759-775.

Butt, N., Campbell, G., Malhi, Y., Morecroft, M., Fenn, K., & Thomas, M., 2009. Initial results from establishment of a long-term broadleaf monitoring plot at Wytham Woods, Oxford, UK. University Oxford, Oxford, UK, Rep.

Calders, K., Origo, N., Burt, A., Disney, M., Nightingale, J., Raunonen, P., Åkerblom, M., Malhi, Y. and Lewis, P., 2018. Realistic Forest Stand Reconstruction from Terrestrial LiDAR for Radiative Transfer Modelling. *Remote Sensing*, 10(6).

Chambers, J. Q., dos Santos, J., Ribeiro, R. J., & Higuchi, N., 2001. Tree damage, allometric relationships, and above-ground net primary production in central Amazon forest. *Forest Ecology and Management*, 152(1), 73-84.

Chave, J., Andalo, C., Brown, S., Cairns, M. A., Chambers, J. Q., Eamus, D., ... & Lescure, J. P., 2005. Tree allometry and improved estimation of carbon stocks and balance in tropical forests. *Oecologia*, 145(1), 87-99.

Chukwu, O., Dau, J.H. and Ezenwenyi, J.U., 2017. Crown-Stump Diameter Model for *Parkia biglobosa* Benth. Species in Makurdi, Benue State, Nigeria. *Journal of Tropical Forestry and Environment*, 7(1).

Coomes, D.A., Dalponte, M., Jucker, T., Asner, G.P., Banin, L.F., Burslem, D.F., Lewis, S.L., Nilus, R., Phillips, O.L., Phua, M.H. and Qie, L., 2017. Area-based vs tree-centric approaches to mapping forest carbon in Southeast Asian forests from airborne laser scanning data. *Remote sensing of environment*, 194, pp.77-88.

Culvenor, D. S. 2003. "Extracting individual tree information: a survey of techniques for high spatial resolution imagery.". In *Remote Sensing of Forest Environments: Concepts and Case Studies*, Edited by: Wulder, M. A and Franklin, S. E (Eds). pp. 255–277. Boston: Kluwer Academic

Dalponte, M., Frizzera, L., Ørka, H.O., Gobakken, T., Næsset, E. and Gianelle, D., 2018. Predicting stem diameters and aboveground biomass of individual trees using remote sensing data. *Ecological indicators*, 85, pp.367-376.

Devi, L. S., & Yadava, P. S., 2009. Aboveground biomass and net primary production of semi-evergreen tropical forest of Manipur, north-eastern India. *Journal of Forestry Research*, 20(2), 151-155.

- Demirbaş, A., 2001. Biomass resource facilities and biomass conversion processing for fuels and chemicals. *Energy conversion and Management*, 42(11), pp.1357-1378.
- Dickinson, Y. L., & Zenner, E. K., 2010. Allometric equations for the aboveground biomass of selected common eastern hardwood understory species. *Northern Journal of Applied Forestry*, 27(4), 160-165.
- Gibbs, H. K., Brown, S., Niles, J. O., & Foley, J. A., 2007. Monitoring and estimating tropical forest carbon stocks: making REDD a reality. *Environmental Research Letters*, 2(4), 045023.
- Gonzalez de Tanago, J., Lau, A., Bartholomeus, H., Herold, M., Avitabile, V., Raumonon, P., Martius, C., Goodman, R.C., Disney, M., Manuri, S. and Burt, A., 2018. Estimation of above-ground biomass of large tropical trees with terrestrial LiDAR. *Methods in Ecology and Evolution*, 9(2), pp.223-234.
- Hashimoto, T., Kojima, K., Tange, T., & Sasaki, S., 2000. Changes in carbon storage in fallow forests in the tropical lowlands of Borneo. *Forest Ecology and Management*, 126(3), 331-337.
- Hunter, M. O., Keller, M., Victoria, D., & Morton, D. C., 2013. Tree height and tropical forest biomass estimation. *Biogeosciences*, 10(12), 8385-8399.
- Lim, K. S., & Treitz, P. M., 2004. Estimation of above ground forest biomass from airborne discrete return laser scanner data using canopy-based quantile estimators. *Scandinavian Journal of Forest Research*, 19(6), 558-570.
- Liu, L., Pang, Y., Li, Z., Si, L., & Liao, S., 2017. Combining Airborne and Terrestrial Laser Scanning Technologies to Measure Forest Understorey Volume. *Forests*, 8(4), 111.
- Lu, D. 2005. Aboveground biomass estimation using Landsat TM data in the Brazilian Amazon Basin.. *International Journal of Remote Sensing*, 26: pp. 2509–2525.
- Montes, N., Gauquelin, T., Badri, W., Bertaudiere, V., & Zaoui, E. H., 2000. A non-destructive method for estimating above-ground forest biomass in threatened woodlands. *Forest Ecology and Management*, 130(1), 37-46.
- Næsset, E., Bollandsas, O.M. and Gobakken, T., 2005. Comparing regression methods in estimation of biophysical properties of forest stands from two different

inventories using laser scanner data.. *Remote Sensing of Environment*, 94: pp. 541–553.

Newnham, G. J., Armston, J. D., Calders, K., Disney, M. I., Lovell, J. L., Schaaf, C. B., ... & Danson, F. M., 2015. Terrestrial laser scanning for plot-scale forest measurement. *Current Forestry Reports*, 1(4), 239-251.

Nordh, N. E., & Verwijst, T., 2004. Above-ground biomass assessments and first cutting cycle production in willow (*Salix* sp.) coppice—a comparison between destructive and non-destructive methods. *biomass and bioenergy*, 27(1), 1-8.

Randle, T., Matthews, R., & Jenkins, T., 2014. Technical Specification for the Biomass Equations Developed for the 2011 Forecast. The Research Agency of the Forestry Commission.

Shrivastava, M. B., & Singh, R. A., 2003. Interrelationships among crown diameter, diameter at breast height and stump diameters of Silver fir trees. In VII World Forestry Congress. Quebec, Canadian. <http://www.fao.org/DOCREP/ARTICLE/WFC/XII/0902-B4.HTM>. Consultado el (Vol. 30).

Solomon, S., Plattner, G.K., Knutti, R. and Friedlingstein, P., 2009. Irreversible climate change due to carbon dioxide emissions. *Proceedings of the national academy of sciences*, 106(6), pp.1704-1709.

Tang, H., Dubayah, R., Swatantran, A., Hofton, M., Sheldon, S., Clark, D. B., & Blair, B., 2012. Retrieval of vertical LAI profiles over tropical rain forests using waveform lidar at La Selva, Costa Rica. *Remote Sensing of Environment*, 124, 242-250.

Team, C.W., Pachauri, R.K. and Meyer, L.A., 2014. IPCC, 2014: climate change 2014: synthesis report. Contribution of Working Groups I. II and III to the Fifth Assessment Report of the intergovernmental panel on Climate Change. IPCC, Geneva, Switzerland, 151.

The Wood Database., 2018. Sycamore Maple, European Ash, and Oak. Retrieved on 23rd August 2017, from <http://www.wood-database.com/>.

Thenkabail, P. S., Stucky, N., Griscom, B. W., Ashton, M. S., Diels, J., van der Meer, B. and Enclona, E., 2004. Biomass estimations and carbon stock calculations in the oil palm plantations of African derived savannas using IKONOS data.. *International Journal of Remote Sensing*, 25: pp. 5447–5472.

Tian, X., Su, Z., Chen, E., Li, Z., van der Tol, C., Guo, J., & He, Q. ,2012. Estimation of forest above-ground biomass using multi-parameter remote sensing data over a cold and arid area. *International journal of applied earth observation and geoinformation*, 14(1), 160-168.

Vashum, K. T., & Jayakumar, S., 2012. Methods to estimate above-ground biomass and carbon stock in natural forests-A review. *J. Ecosyst. Ecogr*, 2(4), 1-7.

Zeidler, A., 2012. Variation of wood density in Turkish hazel (*Corylus colurna* L.) grown in the Czech Republic. *Journal of Forest Science*, 58(4), 145-151.

Zhang, W., Qi, J., Wan, P., Wang, H., Xie, D., Wang, X. and Yan, G., 2016. An easy-to-use airborne LiDAR data filtering method based on cloth simulation. *Remote Sensing*, 8(6), p.501.

9. Appendices

Appendix A. All code for processing the TLS data in this project.

<https://github.com/YuchenGUOGYC/Tree-segmetation-code-offered-by-Hamraz-.git>

Appendix B. LeafData_3Dmodel_metadata.xlsx

Tree_ID	x	y	Volum e_m3	Branch _Lengt h_m.	Heigh t_m	DBH_ cm	DBH_tria ngulation _cm	censu sID	Dead	speci es	leaf_a rea	leaf_a rea_s tart
8109	114.2 73405	193.0 85522	0.082 8	165.27	8.28	7.13	5.32	3935	N	ACER CA	23.5	30.5
8110	112.7 52512	195.8 86661	0.103	138.37	6.59	8.51	6.44	3932	N	ACER CA	19.7	25.6
9	71.29 37276	129.4 05822	12.35	3451.7 7	25.1	94.9	38.2	4252	N	ACER PS	490.5	637.6
29	49.64 10321	107.0 02738	9.868	4020.0 8	24.7	88.6	74	4169	N	ACER PS	571.2	742.6
31	56.68 6152	162.2 04476	7.671	2259.2 5	21	69.1	64.2	4485	N	ACER PS	321.0	417.3
36	67.35 60871	120.5 72091	17.07 5	3985.3 8	26.2	82.9	74.9	4193	N	ACER PS	566.3	736.2
45	47.74 44123	141.5 38188	11.71 6	3111.9 6	23.2	85.8	79.2	4278	N	ACER PS	442.2	574.8
60	42.10 48443	170.7 65049	5.049	1781.1 9	21.5	66.1	57.7	4661	N	ACER PS	253.1	329.0
70	54.87 56836	152.2 60767	5.683	2085.0 9	22.5	64.5	55.8	4481	N	ACER PS	296.3	385.1
82	77.78 61869	173.9 01743	4.425	2237.4 5	20.9	55	49.7	4597	N	ACER PS	317.9	413.3
95	64.82 19583	103.5 41804	7.504	2192.8 8	25.1	69.7	41.6	5838	N	ACER PS	311.6	405.1
137	71.00 45879	126.6 24135	5.981	2721.8 5	24.4	52.4	54.1	4195	N	ACER PS	386.7	502.8
149	109.0 93013	137.8 62185	3.061	1138.1 8	25.2	51.7	45.2	3637	N	ACER PS	161.7	210.2
154	68.71 74956	133.1 81121	3.17	917.14	22.3	47.4	50.6	4253	N	ACER PS	130.3	169.4
156	84.77 52961	149.1 70902	3.749	1327.1 6	23.1	44.9	45.5	4523	N	ACER PS	188.6	245.1
186	91.37 86198	189.2 42805	2.997	1154.1 2	20.5	45.4	36.6	4971	N	ACER PS	164.0	213.2
202	70.06 62166	111.3 03395	8.324	1755.1 5	23.5	78.5	64.9	4190	N	ACER PS	249.4	324.2
203	42.14 99887	182.5 85169	4.232	1866.4 2	21.7	52.3	48.7	4666	N	ACER PS	265.2	344.8
216	82.08 88413	149.4 55041	2.38	988.73	19.6	37.8	37.9	4521	N	ACER PS	140.5	182.6
221	63.57 62921	182.9 14399	6.062	1525.9 3	23.5	55.2	16.7	4619	N	ACER PS	216.8	281.9
223	72.15 64954	182.1 35456	2.455	1267.4 4	21.4	39.5	39.6	4606	N	ACER PS	180.1	234.1
229	72.17 2848	180.2 51151	2.279	1185.8 2	21.7	40.1	40.2	4607	N	ACER PS	168.5	219.0
240	70.14 42385	182.9 541	2.715	981.36	22.5	41.8	41.7	4608	N	ACER PS	139.4	181.3
262	45.70 34683	194.9 62409	4.616	1539.8 5	23.6	61.4	53.7	4849	N	ACER PS	218.8	284.4
283	45.63 22865	126.8 16027	8.252	2042.2 2	20.5	73.3	67.7	4289	N	ACER PS	290.2	377.2
284	104.8 88555	191.8 3921	2.868	1650.7 6	20.2	41	42.3	3909	N	ACER PS	234.6	304.9
286	53.59 25228	118.3 04764	1.765	622.61	20	36.5	37	4178	N	ACER PS	88.5	115.0
291	91.40	161.4	2.046	945.96	19.9	38	37.4	4543	N	ACER	134.4	174.7

	26524	84197								PS		
300	83.30 76244	153.2 92118	2.206	838.16	21.8	41	41.7	4520	N	ACER PS	119.1	154.8
301	125.2 40981	177.0 62773	3.487	2127.5 2	19.5	40.7	41.2	3886	N	ACER PS	302.3	393.0
338	53.73 0719	193.2 64493	6.114	2517.5 6	21.7	62.9	54.3	4865	N	ACER PS	357.7	465.0
350	67.33 94761	135.3 67965	1.482	459.92	21.1	32.8	32.8	4255	N	ACER PS	65.3	85.0
353	50.74 49677	141.5 77078	2.758	937.38	21.2	41.2	41.5	4277	N	ACER PS	133.2	173.1
367	45.60 91192	198.1 88119	1.885	652.4	20.9	37	37.1	4877	N	ACER PS	92.7	120.5
371	83.69 28822	156.1 37741	1.956	703.79	17.3	38.5	38.6	4515	N	ACER PS	100.0	130.0
380	107.0 0751	133.5 1351	1.771	505.41	24.1	35.4	35.6	3644	N	ACER PS	71.8	93.4
386	92.14 95404	137.7 73215	18.30 7	4923.1 5	25.1	86	76.8	4237	N	ACER PS	699.5	909.4
419	105.4 96566	129.6 75715	1.807	784.06	24.6	31.2	31.2	3645	N	ACER PS	111.4	144.8
424	122.7 47172	137.2 11838	1.487	504.67	23.6	32.1	31.8	3614	N	ACER PS	71.7	93.2
439	124.1 3451	151.3 52893	1.907	753.72	23.7	33.4	33.5	3688	N	ACER PS	107.1	139.2
442	123.3 89488	144.0 17878	2.545	656.9	23.7	36.6	37.1	3610	N	ACER PS	93.3	121.3
446	86.73 50212	110.8 75964	65.12 1	11924. 53	30.5	146	127	4197	N	ACER PS	1694. 3	2202. 6
450	124.5 85584	158.3 98569	1.932	829.28	21.9	34	34.1	3692	N	ACER PS	117.8	153.2
469	134.2 5463	129.6 30834	2.03	1039.6 2	23.1	31.5	31.9	3592	N	ACER PS	147.7	192.0
472	76.87 98699	195.3 94801	1.256	509.27	18.9	33.6	33.4	4933	N	ACER PS	72.4	94.1
473	88.82 17647	148.5 26772	1.517	502.15	21.3	31.3	31	4524	N	ACER PS	71.3	92.8
487	88.93 29288	178.3 67776	7.761	3631.8 7	22.2	71.9	67.1	4592	N	ACER PS	516.0	670.9
499	139.8 37304	158.5 75975	1.156	474.02	20.7	30.5	28.9	3706	N	ACER PS	67.4	87.6
501	129.7 11253	129.6 38418	2.159	687.66	21.4	35.1	35.2	3625	N	ACER PS	97.7	127.0
514	69.37 54902	144.6 91225	8.213	0	20.2	82.3	74.9	4256	Y	ACER PS	0.0	0.0
524	138.2 18996	118.4 43796	2.827	1146.8 3	21.7	37.4	37.3	3446	N	ACER PS	162.9	211.8
552	122.9 18359	161.1 94389	1.304	455.16	20.5	32.6	31.9	3694	N	ACER PS	64.7	84.1
562	81.69 01309	182.3 90571	1.012	607.99	17.6	29.3	29.3	4594	N	ACER PS	86.4	112.3
588	65.08 04476	183.2 96533	1.258	343.69	20.9	32.6	32.1	4616	N	ACER PS	48.8	63.5
595	127.3 60018	133.0 47184	2.541	925.24	22.1	36.1	36.2	3621	N	ACER PS	131.5	170.9
596	60.54 36819	128.2 80983	1.053	439.56	18	27.4	27.2	4269	N	ACER PS	62.5	81.2
600	92.20 08163	180.6 90077	4.81	2054.2 9	22.7	60.5	45.6	4588	N	ACER PS	291.9	379.5
602	89.76 39706	157.2 25214	0.884	419.55	19.2	25.3	23.8	4536	N	ACER PS	59.6	77.5
606	110.3 91826	151.7 14638	1.629	830.41	21.5	32.5	32.5	3651	N	ACER PS	118.0	153.4
638	60.84 76427	139.4 48216	1.129	546.83	18	29.1	24.5	4260	N	ACER PS	77.7	101.0
675	109.3 27746	133.0 28779	2.022	423.11	24.8	37.7	37.7	3640	N	ACER PS	60.1	78.2
691	82.78 05166	191.6 68255	1.017	549.2	18.9	29.2	28.9	4949	N	ACER PS	78.0	101.4
700	58.70 13976	124.2 36815	0.812	278.61	17.8	24.1	24.7	4186	N	ACER PS	39.6	51.5

702	125.4 74374	150.3 89328	1.145	488.32	24.3	25.4	24.9	3689	N	ACER PS	69.4	90.2
709	90.85 20201	155.9 44322	0.792	329.54	18.8	26.1	25.6	4535	N	ACER PS	46.8	60.9
710	135.4 88648	104.1 34154	1.174	509.17	16.4	28.3	28.3	6961	N	ACER PS	72.3	94.1
714	89.14 28058	157.8 37111	0.868	683.02	16.7	24.7	25	4537	N	ACER PS	97.0	126.2
752	133.5 14861	133.0 78222	1.863	944.37	20.5	30.9	13.5	3596	N	ACER PS	134.2	174.4
763	107.3 93756	196.9 44664	1.976	968.76	21.4	36.6	36.9	3924	N	ACER PS	137.6	178.9
778	48.13 9064	192.8 72478	3.756	1584.9 3	23.9	47	47.8	4850	N	ACER PS	225.2	292.8
799	89.61 82403	197.8 80644	0.97	409.35	21.9	27	26.4	4964	N	ACER PS	58.2	75.6
827	103.1 51368	136.7 84092	1.334	436.92	24.5	28.9	28.5	4225	N	ACER PS	62.1	80.7
829	112.7 47183	193.1 28024	0.629	319.96	18	23.8	22.7	3931	N	ACER PS	45.5	59.1
834	91.29 30001	150.3 55135	1.297	616.34	20.7	30.6	34.3	4526	N	ACER PS	87.6	113.8
848	114.7 11205	135.4 4778	1.026	218.59	24.7	26.8	26.5	3647	N	ACER PS	31.1	40.4
868	46.14 31633	157.2 41162	0.712	277.43	19.1	22.4	22	4472	N	ACER PS	39.4	51.2
869	74.52 52207	191.4 7911	0.571	261.06	17.2	23.8	10.1	4937	N	ACER PS	37.1	48.2
877	125.6 10001	192.2 76505	1.085	579.54	18.9	27.5	27.6	3949	N	ACER PS	82.3	107.0
913	53.29 14996	120.4 26556	0.642	375.12	16.7	22.7	22.5	4183	N	ACER PS	53.3	69.3
930	116.3 2184	154.3 16985	0.59	233.84	22.8	21.6	18.3	3655	N	ACER PS	33.2	43.2
931	108.8 86457	151.8 49797	0.773	408.91	18	26.4	27.5	3649	N	ACER PS	58.1	75.5
939	129.5 96133	190.1 58396	1.272	673.81	20.1	28.6	28.6	3952	N	ACER PS	95.7	124.5
958	121.0 66886	106.4 417	0.906	328.93	17.2	26.3	25.8	6928	N	ACER PS	46.7	60.8
971	115.6 99052	123.2 86967	0.883	255.03	23.8	24.7	24.4	3399	N	ACER PS	36.2	47.1
977	131.9 15519	101.9 65921	1.521	852.6	13.5	30.6	29.5	6948	N	ACER PS	121.1	157.5
990	103.7 06772	154.9 79824	0.496	212.53	17.1	21.4	21.2	4561	N	ACER PS	30.2	39.3
1014	83.61 4741	194.5 59541	0.475	201.19	18.8	20.3	19.9	4952	N	ACER PS	28.6	37.2
1019	128.7 79146	172.3 87112	3.238	1124.9 2	23.2	45.8	41.6	3867	N	ACER PS	159.8	207.8
1043	67.88 37571	190.3 65579	0.59	457.95	16.7	23	22.3	4938	N	ACER PS	65.1	84.6
1055	53.68 13876	187.6 67947	0.704	348.47	21.6	21.2	20.9	4862	N	ACER PS	49.5	64.4
1081	42.85 73303	103.8 19385	0.706	252.51	20.8	21.8	21.5	5832	N	ACER PS	35.9	46.6
1090	57.27 30995	113.5 58814	0.791	337.49	18.8	25.6	22.2	4175	N	ACER PS	48.0	62.3
1093	132.4 58111	178.2 56097	1.186	645.37	19	30.5	28.1	3875	N	ACER PS	91.7	119.2
1101	122.1 74458	104.3 49343	0.96	523.42	16.2	26.4	25.9	6927	N	ACER PS	74.4	96.7
1107	112.7 07849	132.7 01123	0.801	227.8	24.5	23	24.1	3641	N	ACER PS	32.4	42.1
1108	121.7 20862	152.4 73645	1.339	697.17	22.7	29.3	28.6	3687	N	ACER PS	99.1	128.8
1116	115.9 92686	133.3 61442	1.079	435.6	24.4	26.8	27	3628	N	ACER PS	61.9	80.5
1118	82.43 17742	190.1 96347	0.426	220.63	18.3	19.8	19.8	4948	N	ACER PS	31.3	40.8
1121	82.95 34504	148.9 02139	0.921	357.7	19.8	24.9	13.7	4522	N	ACER PS	50.8	66.1

1129	100.6 16423	156.8 16726	0.382	220.67	14.1	18.9	18.4	4554	N	ACER PS	31.4	40.8
1147	93.65 46581	194.3 23846	1.625	653.8	20.9	32.5	32.1	4972	N	ACER PS	92.9	120.8
1179	87.27 92402	199.0 09188	0.51	308.69	20.5	22	21.9	4963	N	ACER PS	43.9	57.0
1183	122.1 44253	175.7 81002	0.991	353.32	20	26.4	26.6	3882	N	ACER PS	50.2	65.3
1236	80.26 82656	145.1 05715	0.668	537.27	16.7	19.9	20	4246	N	ACER PS	76.3	99.2
1252	132.5 44133	132.8 29573	0.57	195.79	19.3	21.2	17.8	3595	N	ACER PS	27.8	36.2
1254	118.0 06872	143.3 67858	0.679	215.72	21.1	22.9	22.5	3632	N	ACER PS	30.7	39.8
1271	60.54 96461	128.9 33184	0.313	157.51	15.4	15.2	15.1	4268	N	ACER PS	22.4	29.1
1296	120.4 69676	142.5 7618	1.818	985.2	23	31.8	30.9	3612	N	ACER PS	140.0	182.0
1303	102.3 57861	132.7 84855	0.626	421.07	21.2	17.9	20.8	4219	N	ACER PS	59.8	77.8
1312	122.5 78653	167.7 61659	0.454	145.81	18.6	20.6	19.4	3864	N	ACER PS	20.7	26.9
1314	140.0 43162	164.3 55588	0.639	309.71	18	23.1	22.9	3703	N	ACER PS	44.0	57.2
1317	114.1 38635	156.1 17741	2.752	1133.6 9	21.3	38	38.2	3656	N	ACER PS	161.1	209.4
1324	82.08 62569	176.3 12522	0.312	330.85	13.9	15.3	15.6	4593	N	ACER PS	47.0	61.1
1339	58.20 00041	124.9 59496	0.361	195.23	15.5	14.7	14.6	4187	N	ACER PS	27.7	36.1
1344	129.3 96916	163.3 6804	0.544	441.65	15.8	17.9	17.5	3700	N	ACER PS	62.8	81.6
1359	58.45 8771	120.4 20229	0.325	239.47	14.6	13.9	14.2	4185	N	ACER PS	34.0	44.2
1366	115.0 0048	156.8 58547	2.787	919.36	23.1	40.4	41	3657	N	ACER PS	130.6	169.8
1370	138.1 79958	111.7 01874	0.674	245.71	20	19.2	18.9	6955	N	ACER PS	34.9	45.4
1391	119.8 72941	174.6 82596	3.102	1162.7	22.3	51	45.7	3885	N	ACER PS	165.2	214.8
1395	101.6 0863	131.1 55393	0.663	228.03	21.5	20.7	20.3	4218	N	ACER PS	32.4	42.1
1399	109.2 97099	195.3 62962	0.817	440.64	19.8	25.7	25	3927	N	ACER PS	62.6	81.4
1412	119.2 94273	115.0 06512	0.783	497.96	15.6	23.6	23.4	3413	N	ACER PS	70.8	92.0
1417	73.21 94011	160.0 64612	0.28	369.83	13.5	14.5	11.5	4500	N	ACER PS	52.5	68.3
1427	134.8 86808	165.7 86917	0.302	314.47	14.7	14.1	13.9	3702	N	ACER PS	44.7	58.1
1428	49.57 39925	188.0 64603	5.009	1932.7 5	23.3	60.4	12.2	4856	N	ACER PS	274.6	357.0
1466	103.8 77079	149.5 86868	0.224	113.23	19.3	14.4	14.4	4567	N	ACER PS	16.1	20.9
1471	123.9 02437	110.5 7345	0.802	355.63	15.3	22.3	21.8	6929	N	ACER PS	50.5	65.7
1482	125.5 77894	153.6 43597	0.348	162.05	20.7	18.4	21.2	3693	N	ACER PS	23.0	29.9
1484	122.6 5493	165.2 30173	0.892	331.56	19.7	29.6	29.1	3695	N	ACER PS	47.1	61.2
1496	91.74 30331	151.5 59677	1.238	442.55	19.1	30.8	30.6	4529	N	ACER PS	62.9	81.7
1520	61.75 57452	138.1 48176	0.169	48.09	16	13.8	15.3	4262	N	ACER PS	6.8	8.9
1551	128.0 79745	159.0 28767	0.295	262.29	14	17.9	18	3720	N	ACER PS	37.3	48.4
1575	66.10 95347	172.3 87682	0.263	368.28	14.5	14.1	14	4633	N	ACER PS	52.3	68.0
1604	109.5 16733	127.7 89625	1.314	338.74	25.1	30.5	30	3395	N	ACER PS	48.1	62.6
1623	110.3 19855	160.1 51546	0.303	144.43	17.7	17.4	17.3	3661	N	ACER PS	20.5	26.7

1638	126.1 53465	201.7 38969	0.31	207.9	14.6	15.4	15.1	3971	N	ACER PS	29.5	38.4
1661	60.39 10382	120.9 8139	0.080 5	54.14	11.5	10	5.13	4191	N	ACER PS	7.7	10.0
1670	103.1 82089	182.8 69923	4.56	2698.2 5	20.3	57.8	52	4579	N	ACER PS	383.4	498.4
1685	129.0 46165	114.6 922	0.499	425.11	15.1	17.9	16.6	3428	N	ACER PS	60.4	78.5
1713	108.6 44694	189.5 75232	0.086 2	117.55	10.1	10.3	9.81	3930	N	ACER PS	16.7	21.7
1730	45.57 26606	178.3 9927	0.298	197.12	16.8	15.5	16.6	4659	N	ACER PS	28.0	36.4
1747	118.0 93973	106.2 78932	1.552	467.16	21.1	33.7	34.1	6897	N	ACER PS	66.4	86.3
1750	93.03 2748	153.5 54322	1.34	519.48	18.2	32.8	32.1	4530	N	ACER PS	73.8	96.0
1768	113.8 4025	120.7 20251	0.341	245.17	16.8	13.1	12.8	3402	N	ACER PS	34.8	45.3
1777	101.6 42122	195.3 20067	0.168	128.61	15.7	13.2	12.8	4984	N	ACER PS	18.3	23.8
1788	69.00 8875	135.7 54718	0.35	244.22	16.9	16.1	16.3	4254	N	ACER PS	34.7	45.1
1807	93.69 38393	127.9 52589	0.715	353.16	22.1	20.3	19.2	4241	N	ACER PS	50.2	65.2
1808	112.0 22646	119.3 32742	0.922	260.4	21.7	25.6	13.9	3403	N	ACER PS	37.0	48.1
1821	48.77 55622	112.7 03918	0.272	189.82	12.9	14	12.1	4189	N	ACER PS	27.0	35.1
1824	97.23 42131	152.8 60853	0.466	211.26	17.3	20.4	19.6	4563	N	ACER PS	30.0	39.0
1826	91.73 71635	193.1 59632	2.016	626.53	20.4	39.1	39.3	4965	N	ACER PS	89.0	115.7
1832	109.9 11612	164.5 02112	0.148	60.75	9.46	14.1	13.4	3671	N	ACER PS	8.6	11.2
1847	81.61 87619	192.0 98134	0.15	91.27	12.4	13.5	13.9	4950	N	ACER PS	13.0	16.9
1859	117.0 76087	139.0 56986	1.714	602.72	23	34.1	33.5	3631	N	ACER PS	85.6	111.3
1862	76.79 26998	197.6 84314	0.028 6	55.13	7.32	5.76	3.4	4931	N	ACER PS	7.8	10.2
1871	113.7 44016	188.7 57648	0.45	289.21	18.5	20.4	18.8	3929	N	ACER PS	41.1	53.4
1880	127.7 2354	189.6 89942	0.635	368.48	18.2	22.5	22.5	3951	N	ACER PS	52.4	68.1
1914	104.1 07974	169.2 7836	0.138	201.26	10.9	7.43	4.94	4574	N	ACER PS	28.6	37.2
1918	59.59 24031	145.9 83134	0.603	310.96	19.1	19.1	19.5	4259	N	ACER PS	44.2	57.4
1920	110.8 52424	165.8 12973	0.341	224.39	16.1	17.2	17.4	3672	N	ACER PS	31.9	41.4
1923	127.8 78772	175.8 77319	0.264	168.78	15.4	15.6	15.1	3878	N	ACER PS	24.0	31.2
1924	44.07 227	141.0 62672	0.079 2	0	9.63	13.2	12.6	4281	Y	ACER PS	0.0	0.0
1927	114.9 63745	195.1 60106	0.555	235.28	18.9	22	21.9	3933	N	ACER PS	33.4	43.5
1948	81.05 53702	184.7 43622	0.226	113.56	16.1	14.7	14.8	4596	N	ACER PS	16.1	21.0
1970	80.47 49035	196.4 51774	0.303	109.01	19.2	16.8	16.7	4953	N	ACER PS	15.5	20.1
1972	122.2 7755	196.2 10153	0.633	617.25	17.2	19.6	19.2	3947	N	ACER PS	87.7	114.0
1975	140.2 27476	146.4 75181	0.045 1	68.41	7.93	7.61	3.77	3580	N	ACER PS	9.7	12.6
1988	136.8 20111	108.2 43057	1.298	607.37	16.6	28.6	28.9	6958	N	ACER PS	86.3	112.2
2022	56.35 48965	173.0 74638	0.051 9	92.03	9.2	8.19	6.45	4642	N	ACER PS	13.1	17.0
2033	75.13 81817	192.4 71379	0.084 4	89.66	11.5	9.96	9.8	4936	N	ACER PS	12.7	16.6
2040	133.4 55172	190.8 23004	0.28	351.28	14.4	15.6	15.5	3954	N	ACER PS	49.9	64.9

2063	62.32 56141	104.6 3405	0.463	412.26	18.2	16.8	16.1	5837	N	ACER PS	58.6	76.1
2077	127.1 55018	193.3 96347	0.194	171.98	11.4	14.2	14	3968	N	ACER PS	24.4	31.8
2087	53.11 32811	171.9 67219	0.248	223.03	15.2	13.8	12.9	4646	N	ACER PS	31.7	41.2
2091	46.29 06439	180.5 53825	0.166	132.26	14.9	11.9	12.3	4658	N	ACER PS	18.8	24.4
2160	58.78 56235	104.1 98801	0.34	196.2	17.9	16.1	16	5836	N	ACER PS	27.9	36.2
2176	42.12 49481	179.1 2101	0.070 2	71.22	13.3	7.74	6.47	4663	N	ACER PS	10.1	13.2
2193	94.38 60143	165.8 04491	0.038 5	78.61	4.89	6.34	6.81	4548	N	ACER PS	11.2	14.5
2215	79.52 41091	192.3 02446	0.033 4	43.36	7.59	8.14	7.58	4934	N	ACER PS	6.2	8.0
2225	119.0 39222	156.8 2406	0.266	160.39	14.4	16.2	15.2	3682	N	ACER PS	22.8	29.6
2227	127.1 70495	104.1 51562	0.568	280.33	14.7	19.9	21.7	6935	N	ACER PS	39.8	51.8
2232	55.60 6904	189.6 77146	0.032 8	79.9	8.58	7.1	6.77	4863	N	ACER PS	11.4	14.8
2240	52.28 48892	185.3 86202	0.057 6	98.39	9.26	7.78	8.13	4654	N	ACER PS	14.0	18.2
2262	57.22 21636	121.1 13733	0.43	214.41	17.5	16.4	16.4	4184	N	ACER PS	30.5	39.6
2267	122.5 64636	166.9 65572	0.069 7	23.71	10.3	10.2	11.2	3863	N	ACER PS	3.4	4.4
2290	139.2 5764	144.4 26103	0.341	448.88	13	14	13.9	3582	N	ACER PS	63.8	82.9
2308	87.20 54433	167.8 80108	0.018 1	24.66	9.01	6.26	3.83	4578	N	ACER PS	3.5	4.6
2323	128.0 709	194.7 88778	0.055 5	84.96	11.1	8.08	8	3967	N	ACER PS	12.1	15.7
2350	85.86 62866	132.8 31721	0.205	232.7	10.8	12.9	12.2	4242	N	ACER PS	33.1	43.0
2351	74.72 91366	161.9 59783	0.204	302.3	13.4	11.4	11.5	4507	N	ACER PS	43.0	55.8
2361	89.81 41194	157.9 85687	0.042 5	0	6.58	10.2	6.73	4538	Y	ACER PS	0.0	0.0
8011	111.7 89881	111.7 57621	0.172	169.82	10.2	11.9	11.9	3410	N	ACER PS	24.1	31.4
8013	111.5 78192	104.8 57744	0.181	124.57	13.8	12.7	1.02	6881	N	ACER PS	17.7	23.0
8014	125.0 48736	112.0 7397	0.377	222.92	16	15.4	16.6	6930	N	ACER PS	31.7	41.2
8018	93.66 90403	197.4 77702	0.047 9	94.66	9.85	8.89	10.2	4988	N	ACER PS	13.4	17.5
8019	94.53 70478	192.3 42792	0.942	479.47	21.8	28.1	27.2	4973	N	ACER PS	68.1	88.6
8020	122.9 72232	196.3 83037	0.036 9	77.7	6.65	5.79	5.1	3948	N	ACER PS	11.0	14.4
8021	131.3 68304	193.9 24473	0.051 9	90.87	10.3	7.88	8.87	3955	N	ACER PS	12.9	16.8
8023	119.3 27174	189.6 1076	0.049 3	88.64	8.09	6.74	5.79	3938	N	ACER PS	12.6	16.4
8024	115.4 53967	185.5 58783	0.062 2	80.64	10.7	8.01	8	3888	N	ACER PS	11.5	14.9
8025	122.3 33162	157.2 40405	0.026 8	0	3.75	10.6	10.6	3685	Y	ACER PS	0.0	0.0
8030	52.22 46344	107.2 77075	0.021	33.92	3.09	5.82	7.42	4170	N	ACER PS	4.8	6.3
8031	55.94 14015	118.1 84958	0.08	112.37	9.32	8.81	8.52	4177	N	ACER PS	16.0	20.8
8035	42.98 64513	138.6 22988	0.105	84.02	12.4	10	5.34	4283	N	ACER PS	11.9	15.5
8042	101.8 0037	101.6 82491	0.033 1	58.45	8.19	7.36	6.58	6874	N	ACER PS	8.3	10.8
8054	122.6 59742	103.9 07384	0.010 4	19.77	4.83	4.65	4.12	NA	N	ACER PS	2.8	3.7
8055	121.5 21802	104.1 02832	0.012	14.59	6.41	5.48	5.75	6926	N	ACER PS	2.1	2.7

8059	138.6 60936	115.0 25711	0.413	276.5	16.4	16.5	15.8	3447	N	ACER PS	39.3	51.1
8066	93.33 51571	127.1 05742	0.18	258.08	10.5	9.45	9.42	4204	N	ACER PS	36.7	47.7
8067	93.84 44533	126.9 14704	0.089 9	156.22	9.39	7.48	8.11	4205	N	ACER PS	22.2	28.9
8072	61.21 71351	127.9 72894	0.112	116.47	13.2	9.5	6.6	4270	N	ACER PS	16.5	21.5
8073	60.93 58848	129.3 37262	0.049 3	59.33	6.54	7.99	4.18	4267	N	ACER PS	8.4	11.0
8074	82.37 34009	139.7 60056	0.453	329.94	15.7	16.7	16.6	4243	N	ACER PS	46.9	60.9
8083	62.25 27993	139.0 72924	0.085 1	132.53	7.97	7.14	5.1	4261	N	ACER PS	18.8	24.5
8096	55.43 73382	195.6 89709	0.008 04	15.49	5.42	3.8	5.82	4868	N	ACER PS	2.2	2.9
8098	52.02 35654	187.6 68676	0.010 4	17.18	6.7	4.05	3.78	4861	N	ACER PS	2.4	3.2
8111	109.2 80615	192.3 50734	0.022 9	55.57	5.16	4.98	2.92	3928	N	ACER PS	7.9	10.3
8117	81.96 55639	193.9 8316	0.105	126.43	12.8	10.7	13	4951	N	ACER PS	18.0	23.4
8126	88.39 53895	182.8 20872	0.373	141.76	15.6	19.1	19.3	4591	N	ACER PS	20.1	26.2
8127	87.35 44384	185.3 68572	0.036 1	82.77	7.41	6.21	3.03	4590	N	ACER PS	11.8	15.3
8128	82.21 98596	183.4 85492	0.012 8	23.56	3.85	4.21	3.86	4595	N	ACER PS	3.3	4.4
8140	74.59 25818	161.4 64728	0.044 5	78.18	8.02	5.71	4.69	4506	N	ACER PS	11.1	14.4
8142	73.90 28513	160.4 04948	0.082 6	136.82	6.39	8.72	7.85	4501	N	ACER PS	19.4	25.3
8150	87.78 68506	167.8 91019	0.047 9	65.05	9.69	8.52	8.51	4577	N	ACER PS	9.2	12.0
8164	103.8 51114	146.9 93207	0.077 7	69.19	12.2	8.8	3.63	4231	N	ACER PS	9.8	12.8
8167	103.6 60837	148.4 58735	0.011 1	16.66	5.76	4.83	4.77	4569	N	ACER PS	2.4	3.1
8168	103.8 36392	150.1 44172	0.012 5	19.86	5.81	4.84	3.76	4566	N	ACER PS	2.8	3.7
8171	103.0 88127	152.7 74467	0.017 9	0	8.32	6.39	6.34	4562	Y	ACER PS	0.0	0.0
8174	109.7 80598	160.7 04982	0.045 5	92.66	4.64	6.63	6.26	3662	N	ACER PS	13.2	17.1
8179	134.8 69994	168.3 269	0.007 57	10.72	2.86	3.87	2.49	3856	N	ACER PS	1.5	2.0
8180	133.3 45106	167.4 88692	0.033 3	46.91	6.63	6.1	6.01	3857	N	ACER PS	6.7	8.7
8182	129.3 19166	174.0 99268	0.035 2	68.19	8.41	5.99	11.3	3877	N	ACER PS	9.7	12.6
8190	131.1 68635	166.1 60401	0.199	130.33	13.3	15.2	14.6	3860	N	ACER PS	18.5	24.1
8198	117.7 58287	152.3 74295	1.042	356.41	22.7	27.2	27.3	3653	N	ACER PS	50.6	65.8
8201	131.4 34316	153.6 83175	0.16	192.57	11.8	9.97	9.65	3718	N	ACER PS	27.4	35.6
8203	139.8 75828	145.3 6194	0.017 3	26.92	8.07	5.64	4.57	3581	N	ACER PS	3.8	5.0
8219	132.2 52375	142.5 64324	0.694	460.46	20.5	19.8	19.2	3606	N	ACER PS	65.4	85.1
8223	104.9 28825	146.3 4017	0.013 1	16.66	5.84	5.36	4.15	3634	N	ACER PS	2.4	3.1
8500	75.79 34812	191.7 09704	0.36	208.86	17.3	18.4	15.2	4935	N	ACER PS	29.7	38.6
9088	59.50 94922	114.1 08624	0.258	285.91	13.8	12.8	12.4	4176	N	ACER PS	40.6	52.8
9091	71.25 0341	156.9 25345	0.059 6	83.51	10.1	7.65	7.6	4497	N	ACER PS	11.9	15.4
9095	48.30 07209	159.3 16985	0.060 3	88.25	8.48	8.47	8.35	4476	N	ACER PS	12.5	16.3
9100	56.48 60605	198.4 74892	0.014 3	0	4.59	7.12	7.02	4871	Y	ACER PS	0.0	0.0

9108	44.51 70558	185.2 72207	0.077 7	0	9.93	9.06	8.88	4668	Y	ACER PS	0.0	0.0
9228	125.5 63157	119.5 60953	0.396	276.3	15.4	16.2	6.2	3426	N	ACER PS	39.3	51.0
9230	118.5 84615	157.5 73498	1.936	751.96	22.7	33.9	35.6	3681	N	ACER PS	106.8	138.9
9231	121.6 08667	157.8 98742	0.538	200.15	21.9	16.1	5.86	3684	N	ACER PS	28.4	37.0
9232	117.4 06537	193.0 73168	0.205	268.59	13	12.6	12.4	3937	N	ACER PS	38.2	49.6
1009a	110.5 17913	112.7 97542	0.811	283.98	21.3	21.7	23.8	3408	N	ACER PS	40.3	52.5
1009b	110.8 80404	112.7 82852	0.98	431.34	20.7	23.5	23.2	3409	N	ACER PS	61.3	79.7
1075a	48.26 14284	135.9 14004	1.323	406.46	20.2	29.4	28.5	4280	N	ACER PS	57.8	75.1
1075b	48.88 91272	136.1 98183	0.619	279.22	19.3	22.1	21.3	4279	N	ACER PS	39.7	51.6
1087a	141.4 08167	162.2 70462	1.036	420.75	18.8	29	25.5	3722	N	ACER PS	59.8	77.7
1087b	141.4 69626	162.7 25349	0.671	283.53	17.3	22.2	21.7	3723	N	ACER PS	40.3	52.4
1135b	97.35 0357	98.03 3737	0.147	129.98	10	7.69	4.03	5877	N	ACER PS	18.5	24.0
1195a	55.48 45594	136.0 69462	0.82	311.37	19.7	24.6	24	4275	N	ACER PS	44.2	57.5
1195b	55.05 39198	136.2 55412	0.036 4	12.79	6.74	9.37	8.16	4267	N	ACER PS	1.8	2.4
1195c	56.16 22122	136.4 92292	0.102	47.78	12.4	11.8	12.2	4274	N	ACER PS	6.8	8.8
1278a	113.1 8484	120.9 74338	1.26	718.95	19.1	28.9	26	3400	N	ACER PS	102.2	132.8
1278b	113.4 90435	121.1 56748	0.288	170.97	17.9	15.7	15.1	3401	N	ACER PS	24.3	31.6
138a	55.55 91428	111.1 9103	2.012	484.19	23.6	45.1	14.6	4172	N	ACER PS	68.8	89.4
138b	55.55 29501	110.9 31678	2.116	562.68	23.6	37.8	30.8	4171	N	ACER PS	79.9	103.9
139a	92.93 6466	123.6 68663	4.913	1262.5 9	26.6	53.9	48.3	4207	N	ACER PS	179.4	233.2
139b	92.55 42528	123.7 35596	0.042 4	49.97	5.08	6.99	4.53	4206	N	ACER PS	7.1	9.2
1438a	54.62 23335	196.5 95399	0.081 4	100.79	10.5	9.33	12.2	4869	N	ACER PS	14.3	18.6
1438b	55.04 40496	196.7 0576	0.213	215.53	14.2	16.1	17.2	4870	N	ACER PS	30.6	39.8
1480a	138.3 53357	157.2 0188	0.181	160.61	12.1	13.6	5.06	3710	N	ACER PS	22.8	29.7
1480b	138.9 44484	156.6 97737	0.237	193.58	12.6	14.6	11.2	3711	N	ACER PS	27.5	35.8
1480c	138.8 9721	157.1 4399	1.339	889.4	20.2	25.6	6.01	3712	N	ACER PS	126.4	164.3
1480d	138.3 13133	157.5 95352	0.237	190.43	14	15	7.34	3709	N	ACER PS	27.1	35.2
1480e	139.6 93867	156.8 92497	0.025 5	4.83	4.14	8.61	7.35	3713	N	ACER PS	0.7	0.9
1501a	43.61 4043	103.6 13319	0.444	175.04	18.1	19.2	11.2	5834	N	ACER PS	24.9	32.3
1501b	43.33 51636	103.7 21588	0.502	198.74	20.3	19.6	28.5	5833	N	ACER PS	28.2	36.7
1513a	116.2 08073	127.6 74012	1.232	340.59	24.4	27.9	28	3398	N	ACER PS	48.4	62.9
1513b	116.0 59306	127.3 68741	0.149	59.65	15.1	8.53	5.07	3397	N	ACER PS	8.5	11.0
1532a	53.53 93981	171.7 5727	0.415	303.5	14.8	17.9	23.6	4645	N	ACER PS	43.1	56.1
1532b	53.63 70899	172.2 16308	0.097 3	108.38	10.2	11	10.9	4644	N	ACER PS	15.4	20.0
1570a	108.8 86478	131.6 03763	1.938	536.37	25.6	32.5	28.9	3643	N	ACER PS	76.2	99.1
1570b	108.9 62422	131.1 693	0.561	224.2	22.8	18.6	18.7	3642	N	ACER PS	31.9	41.4

1581a	126.9 4332	151.4 38027	0.06	0	11.7	10.7	10.4	3690	Y	ACER PS	0.0	0.0
1581b	126.8 41383	151.7 93354	0.729	210.55	23.5	24.2	22.7	3691	N	ACER PS	29.9	38.9
1593a	104.6 37356	167.6 91631	0.323	298.15	14.6	14.9	5.71	4573	N	ACER PS	42.4	55.1
1593b	103.8 43175	168.3 27796	0.053 4	6.39	5.42	12	11.8	4570	N	ACER PS	0.9	1.2
1593c	104.0 25631	167.7 67314	0.399	357.46	15.5	15.4	9.11	4571	N	ACER PS	50.8	66.0
1593d	104.1 91918	167.6 39884	0.228	139.29	12.3	15.7	7.61	4572	N	ACER PS	19.8	25.7
1679a	133.7 18305	109.2 07413	0.404	260.53	14.7	13.8	12.6	6959	N	ACER PS	37.0	48.1
1679b	132.8 32557	109.7 14328	0.024 9	0	2.93	4.75	2.77	NA	Y	ACER PS	0.0	0.0
174a	63.64 95182	154.8 02983	3.388	1653.4 3	22	44	45.2	4489	N	ACER PS	234.9	305.4
174b	64.26 37546	154.8 06254	0.193	154.32	11.6	14.7	5.94	4488	N	ACER PS	21.9	28.5
1800a	108.8 01903	105.7 93448	0.597	236.7	21.1	18.5	18.1	6880	N	ACER PS	33.6	43.7
1800b	109.1 99036	105.5 69545	0.203	144.85	13.4	12	11.9	6879	N	ACER PS	20.6	26.8
180a	111.8 45716	137.1 23643	3.139	874.86	25.5	53.6	44.3	3639	N	ACER PS	124.3	161.6
180b	111.4 80044	137.8 14174	0.007 54	10.46	3.53	4.41	1.62	NA	N	ACER PS	1.5	1.9
184a	96.10 5175	130.4 47564	2.503	687.51	26.2	46.7	48.1	4240	N	ACER PS	97.7	127.0
184b	96.27 52707	130.0 13756	0.064	0	7.23	13.2	2.88	4239	Y	ACER PS	0.0	0.0
184c	96.54 01041	130.6 27688	0.058 2	0	4.56	13.8	13.7	4238	Y	ACER PS	0.0	0.0
1861a	110.7 77278	163.7 98686	0.655	447.32	18	21.8	22.4	3669	N	ACER PS	63.6	82.6
1861b	110.4 45197	163.4 54863	0.081 5	82.95	9.36	6.56	2.36	3670	N	ACER PS	11.8	15.3
2006a	107.4 81677	147.9 30252	0.064 1	86.06	9.77	7.56	7.7	3636	N	ACER PS	12.2	15.9
2006b	107.3 66853	147.4 8308	0.243	306.86	15.2	12.3	11.9	3635	N	ACER PS	43.6	56.7
201a	96.32 01408	150.6 1483	1.95	876.73	19.1	35.2	11.8	4564	N	ACER PS	124.6	161.9
201b	96.61 22358	150.2 14474	1.79	742.24	19	35.9	18.7	4565	N	ACER PS	105.5	137.1
2049a	53.30 70286	173.9 38779	0.422	405.82	15.5	17.3	21.1	4649	N	ACER PS	57.7	75.0
213a	115.2 41125	129.9 33305	1.218	409.14	24.4	30.6	28.9	3627	N	ACER PS	58.1	75.6
213b	115.4 4186	130.2 03882	3.189	937.42	25.1	40.5	44.2	3626	N	ACER PS	133.2	173.2
250a	40.94 1905	108.2 73286	1.436	436.62	21.7	28	18.6	4149	N	ACER PS	62.0	80.6
255a	85.42 11076	126.9 13401	0.394	183.87	12.6	21.5	13.6	4198	N	ACER PS	26.1	34.0
255b	86.08 72306	126.8 50131	0.364	227.48	18.4	15.8	15.8	4202	N	ACER PS	32.3	42.0
255c	86.06 69804	127.2 33171	3.37	891.53	25.8	45.6	45.4	4201	N	ACER PS	126.7	164.7
255d	85.68 85282	127.8 54586	2.376	715.94	25.9	36.4	36.7	4200	N	ACER PS	101.7	132.2
255e	85.45 69905	127.4 30148	1.84	799.08	22.6	35.6	23.3	4199	N	ACER PS	113.5	147.6
324a	51.74 08015	118.7 61682	0.171	72.13	10.8	17	16.2	4180	N	ACER PS	10.2	13.3
324b	51.94 5779	118.4 46611	0.896	438.73	16.4	26.9	25.6	4179	N	ACER PS	62.3	81.0
330a	68.65 30087	157.5 43198	0.078 4	101.34	8.44	8.85	5.94	4492	N	ACER PS	14.4	18.7
330b	68.20 89626	157.2 86998	0.021 7	27.03	3.39	7.86	8.24	4491	N	ACER PS	3.8	5.0

330c	68.36 5056	156.9 2902	1.787	731.74	21.9	34.2	34.4	4490	N	ACER PS	104.0	135.2
330d	68.68 58658	156.8 02839	0.8	346.92	20.5	26.2	33.6	4493	N	ACER PS	49.3	64.1
387a	126.3 34439	142.5 93749	2.525	1245.6 4	22.8	36.7	36.4	3608	N	ACER PS	177.0	230.1
387b	125.7 53377	142.2 10424	2.283	881.38	23.7	36.6	36.7	3609	N	ACER PS	125.2	162.8
409a	109.5 02783	118.2 24921	1.481	717.98	20.8	30.3	29.2	3405	N	ACER PS	102.0	132.6
409b	109.4 39367	118.7 49888	0.010 2	15.42	2.84	4.7	4.21	3404	N	ACER PS	2.2	2.8
438a	74.72 0914	157.9 46152	0.131	138.17	11.7	11.4	11	4503	N	ACER PS	19.6	25.5
438b	74.40 73547	158.4 70984	1.137	509.13	19.8	31.4	31.3	4502	N	ACER PS	72.3	94.0
488a	112.2 7474	162.3 08413	2.312	1175.7 5	19.9	39.2	35.3	3664	N	ACER PS	167.1	217.2
488b	112.4 97655	162.0 14279	0.284	140.44	15.4	16.3	16.7	3665	N	ACER PS	20.0	25.9
521a	44.14 17075	150.8 37753	1.011	377.83	21.7	26.8	17.5	4464	N	ACER PS	53.7	69.8
521b	44.52 83655	151.1 83463	1.178	429.63	22	28.8	27.7	4465	N	ACER PS	61.0	79.4
521c	44.49 37438	151.4 30475	1.027	455.88	20.7	27.3	26.6	4466	N	ACER PS	64.8	84.2
599a	81.66 59551	155.1 39412	0.091 9	123.41	8.79	10.1	15.2	4516	N	ACER PS	17.5	22.8
599b	80.92 16793	154.9 45354	0.351	195.36	17.3	17.4	17.2	4517	N	ACER PS	27.8	36.1
599c	81.48 17643	154.1 39636	1.599	605.09	19.6	39.3	34.9	4519	N	ACER PS	86.0	111.8
5a	93.13 48075	162.5 01599	2.712	1341.9 9	21.4	42.8	21.7	4547	N	ACER PS	190.7	247.9
5b	93.02 15018	162.0 07011	2.175	854.15	21.5	38.7	14.7	4546	N	ACER PS	121.4	157.8
5c	92.74 11011	162.4 04518	0.043 4	19.01	5.28	8.58	8.78	4545	N	ACER PS	2.7	3.5
654a	64.16 29052	153.7 55625	0.767	277.59	19.4	24.5	23.5	4486	N	ACER PS	39.4	51.3
654b	64.46 72175	153.6 13729	0.255	97.81	20.2	15.7	15.5	4487	N	ACER PS	13.9	18.1
705a	42.32 16166	139.4 16114	1.002	324.6	19.9	26.1	25.7	4282	N	ACER PS	46.1	60.0
705b	42.44 52964	138.9 4323	0.007 71	0	2.64	7.07	4.17	NA	Y	ACER PS	0.0	0.0
8012a	113.5 44294	112.8 0915	0.54	280.69	15.5	21.8	16.6	3411	N	ACER PS	39.9	51.8
8012b	114.0 27603	112.7 06328	0.474	216	13.9	23.3	22.7	3412	N	ACER PS	30.7	39.9
8028a	49.39 77058	149.2 48391	0.128	167.04	12.3	11.7	10.4	4480	N	ACER PS	23.7	30.9
8028b	49.58 54378	148.9 08493	0.001 45	0	1.9	2.25	2.3	NA	Y	ACER PS	0.0	0.0
8028c	49.82 82275	149.4 79641	0.053 5	85.7	8.62	8.02	7.76	4479	N	ACER PS	12.2	15.8
8049a	119.8 32193	101.2 5485	0.021 4	35.54	7.32	5.78	6.74	6903	N	ACER PS	5.0	6.6
8049b	120.0 72908	101.5 83432	0.023 6	41.91	6.44	4.72	1.99	NA	N	ACER PS	6.0	7.7
8053a	119.1 95271	100.8 73887	0.026 6	34.05	3.95	6.13	5.95	6902	N	ACER PS	4.8	6.3
8053b	120.0 25857	100.8 12046	0.014 9	33.87	4.72	4.21	2.61	6901	N	ACER PS	4.8	6.3
805a	71.80 55859	157.2 5844	1.131	425.75	20	28.5	28.1	4498	N	ACER PS	60.5	78.6
805b	71.80 38142	157.7 2581	0.838	335.87	19	24.4	24.5	4499	N	ACER PS	47.7	62.0
8086a	42.89 35794	180.8 69728	0.071 9	88.4	11.8	7.46	6.56	4664	N	ACER PS	12.6	16.3
8086b	43.20 9515	180.8 472	0.235	229.84	14.2	14.4	15.1	4665	N	ACER PS	32.7	42.5

8099a	52.51 13122	184.9 25309	0.010 7	16.65	4.98	4.43	1.36	NA	N	ACER PS	2.4	3.1
8099c	51.61 17243	185.4 35901	0.018	44.17	7.36	5.82	4.4	NA	N	ACER PS	6.3	8.2
8099d	51.54 01036	184.7 71322	0.021 5	43.66	5.95	4.85	3.64	NA	N	ACER PS	6.2	8.1
8105a	55.74 54638	173.3 81901	0.004 29	5.95	2.72	4.41	2.6	NA	N	ACER PS	0.8	1.1
8105b	55.96 83524	172.8 03054	0.031 9	88.27	9.2	7.24	3.9	4643	N	ACER PS	12.5	16.3
8107b	52.58 00814	173.3 0667	0.193	150.09	14.5	12.6	12.3	4647	N	ACER PS	21.3	27.7
8107c	52.42 9677	173.6 2401	0.147	65.12	11.4	13.1	11.1	4648	N	ACER PS	9.3	12.0
8107d	53.40 57907	173.7 12012	0.063 7	81.12	10.8	8.62	7.3	4650	N	ACER PS	11.5	15.0
8145a	121.8 2819	119.7 82892	0.018 5	33.75	7.86	4.05	1.4	NA	N	ACER PS	4.8	6.2
8145b	121.6 4769	120.1 49437	0.014	17.33	5.79	5.88	13.4	NA	N	ACER PS	2.5	3.2
8145c	121.0 31942	120.2 26697	0.005 64	7.42	4.14	4.24	0.97	NA	N	ACER PS	1.1	1.4
8161a	128.9 03648	132.0 53519	0.011 2	20.44	4.97	3.55	6.4	NA	N	ACER PS	2.9	3.8
8161b	128.9 4034	131.8 80648	0.008 08	19.15	5.25	3.85	3.24	NA	N	ACER PS	2.7	3.5
8169a	104.7 0124	149.5 42899	0.016 2	27.52	7.8	4.41	1.5	NA	N	ACER PS	3.9	5.1
8169b	104.6 75295	149.8 64073	0.045 4	64.32	9.07	6.33	0.96	4568	N	ACER PS	9.1	11.9
817a	130.0 93388	153.2 74235	1.55	753.87	23	30.5	30.2	3719	N	ACER PS	107.1	139.2
817b	129.9 23716	153.8 77965	0.018 1	36.59	3.04	4.84	3.9	NA	N	ACER PS	5.2	6.8
8222a	135.7 16254	129.8 61182	0.048 2	75.88	9.08	4.36	5.9	3591	N	ACER PS	10.8	14.0
8222b	135.5 24755	130.2 52648	0.004 01	0	3.91	4.41	3.5	NA	Y	ACER PS	0.0	0.0
8222c	135.8 8638	130.9 9642	0.044 6	82.11	5.98	4.6	5.49	3590	N	ACER PS	11.7	15.2
8222d	136.6 02748	130.7 4745	(0.080 9+0j)	174.9	(8.76 +0j)	(6.41 +0j)	(nan+na n*)	3589	N	ACER PS	24.9	32.3
893a	64.22 75188	130.4 93451	0.725	258.98	18.2	23.5	24.3	4265	N	ACER PS	36.8	47.8
893b	64.41 81586	130.8 80708	0.695	329.94	18.6	21.9	21.8	4266	N	ACER PS	46.9	60.9
9092a	72.39 69534	155.1 69947	0.182	131	14.4	14.5	14.6	4496	N	ACER PS	18.6	24.2
9092b	72.66 05929	155.3 19804	0.037 8	0	3.6	11.6	12.1	NA	Y	ACER PS	0.0	0.0
9099b	68.63 91892	201.6 69211	0.164	178.54	14.1	12.5	5.2	4919	N	ACER PS	25.4	33.0
9102a	46.55 86294	198.6 29221	0.147	143.58	11.7	13.5	12.9	4876	N	ACER PS	20.4	26.5
9107a	46.57 11572	183.5 8172	0.074 6	57.33	14.1	9.51	8.61	4657	N	ACER PS	8.1	10.6
9107b	46.40 16973	184.2 18276	0.026 9	41.39	8.96	5.93	4.2	4656	N	ACER PS	5.9	7.6
914d	138.9 25163	158.0 33472	1.938	987.49	19.8	34.6	33.9	3715	N	ACER PS	140.3	182.4
914e	138.4 66378	158.5 84382	0.011 9	3.46	1.67	6.96	4.86	3707	N	ACER PS	0.5	0.6
927a	97.74 61188	125.8 31397	0.941	319.46	25.9	23.8	27	4212	N	ACER PS	45.4	59.0
927c	97.88 99829	126.2 32515	0.234	149.77	17.1	12.7	6.4	4213	N	ACER PS	21.3	27.7
927d	97.07 56685	125.7 32135	0.006 92	0	1.86	0.5	12.6	4211	Y	ACER PS	0.0	0.0
927e	97.31 03481	125.3 87877	1.983	572.94	26.9	32.7	32.1	4210	N	ACER PS	81.4	105.8
945a	47.42 79526	155.3 78517	1.159	490.08	20	27.4	27.2	4477	N	ACER PS	69.6	90.5

945b	47.21 41732	155.0 42451	0.578	213.21	19.5	20.8	10.7	4478	N	ACER PS	30.3	39.4
8070	95.03 88775	121.9 72457	0.058 7	195.65	5.7	5.86	7.99	4208	N	COR YAV	27.8	36.1
8082	59.84 97092	135.0 20785	0.189	334.51	7.47	8.63	8	4263	N	COR YAV	47.5	61.8
8084	63.58 77091	146.1 56499	0.196	384.99	7.31	10.8	10.8	4258	N	COR YAV	54.7	71.1
8139	67.05 39846	180.3 37391	0.214	261.42	10.3	13.5	11.7	4614	N	COR YAV	37.1	48.3
8177	100.9 13601	135.2 6118	0.050 1	140.07	5.85	6.37	9.12	4221	N	COR YAV	19.9	25.9
8193	112.5 54686	169.2 09297	0.261	318.94	11.2	10.3	8.04	NA	N	COR YAV	45.3	58.9
8206	117.6 88913	135.2 51386	0.177	319.05	7.51	9.17	8.22	3629	N	COR YAV	45.3	58.9
8207	127.2 1718	123.2 56272	0.227	236.8	10.7	10.5	10.1	3422	N	COR YAV	33.6	43.7
1822a	75.69 22624	183.6 52399	0.125	186.78	10.7	8.65	8.78	4605	N	COR YAV	26.5	34.5
1822b	75.97 68362	184.1 52666	0.089 7	360.69	6.04	9.87	3.49	4599	N	COR YAV	51.2	66.6
1822c	75.66 69926	183.3 72488	0.209	328.93	9.67	10.7	6.05	4602	N	COR YAV	46.7	60.8
1822d	76.05 57345	183.3 68918	0.042 1	158.49	7.46	4.72	4.76	4600	N	COR YAV	22.5	29.3
1822e	75.92 75357	183.4 07038	0.253	328.97	12.1	9.46	4.57	4601	N	COR YAV	46.7	60.8
8061a	132.3 85611	106.1 80131	0.243	296.99	12	11	3.04	6949	N	COR YAV	42.2	54.9
8061b	132.0 91806	105.8 77978	0.091 4	112	8.74	8.19	4.43	6950	N	COR YAV	15.9	20.7
8061c	132.0 50792	106.5 28516	0.006 57	0	1.63	7.4	6.62	NA	Y	COR YAV	0.0	0.0
8061d	131.8 05089	106.2 18271	0.002 06	0	0.89	0.5	6.19	NA	Y	COR YAV	0.0	0.0
8071b	95.45 6764	122.1 83536	0.121	257.42	9.75	7.16	5.85	4209	N	COR YAV	36.6	47.5
8075a	104.3 87431	120.5 35906	0.12	187.32	6.65	6.42	7.32	NA	N	COR YAV	26.6	34.6
8075b	104.3 02518	119.7 22688	0.143	246.56	6	8.27	7.72	NA	N	COR YAV	35.0	45.5
8079a	107.3 6393	123.6 9754	0.022 9	56.83	6.19	6.05	1.08	3394	N	COR YAV	8.1	10.5
8079b	107.1 26001	123.3 89771	0.067 2	134.36	6.4	7.39	5.2	3393	N	COR YAV	19.1	24.8
8118b	62.38 88888	197.3 95796	0.063 3	119.02	6.16	5.77	1.97	4947	N	COR YAV	16.9	22.0
8118c	62.91 42852	197.1 43215	0.395	404.4	10.9	12.7	22.5	4945	N	COR YAV	57.5	74.7
8118d	62.69 86913	197.1 22991	0.416	441.29	14.4	15.5	23.3	4944	N	COR YAV	62.7	81.5
8138a	69.45 34745	181.0 60533	0.137	102.04	8.12	16	18.7	NA	N	COR YAV	14.5	18.8
8138b	69.76 3028	180.7 73534	0.317	528.9	11.5	11.4	9.08	NA	N	COR YAV	75.1	97.7
8159a	91.80 03909	153.9 80959	0.131	174.26	7.64	10.3	6.41	4534	N	COR YAV	24.8	32.2
8159b	91.40 32733	154.3 93637	0.083 5	167.83	5.03	7	7.5	4532	N	COR YAV	23.8	31.0
8159c	91.46 33595	153.9 34557	0.133	206.11	8.29	8.48	2.26	4531	N	COR YAV	29.3	38.1
8159d	91.79 69079	154.2 62563	0.103	154.6	6.47	7.51	5.94	4533	N	COR YAV	22.0	28.6
8172a	103.7 09942	157.2 15079	0.102	113.42	7.56	7.85	3.36	NA	N	COR YAV	16.1	21.0
8172c	104.6 12631	157.2 47863	0.024	16.56	5.26	6.39	6.55	NA	N	COR YAV	2.4	3.1
8172d	104.2 6464	157.0 47613	0.184	160.37	10.9	11.1	9.01	NA	N	COR YAV	22.8	29.6
8172f	103.8 65814	156.9 96107	0.124	197.72	10.1	8.35	0.76	NA	N	COR YAV	28.1	36.5

2312	69.59 9442	173.0 4258	0.379	554.28	10.8	10.4	10.1	4635	N	CRAT MO	78.8	102.4
8015	127.7 16928	110.0 09532	0.047 8	73.74	5.14	7.32	6.24	6933	N	CRAT MO	10.5	13.6
8022	128.4 08123	198.5 74868	0.268	431.3	8.27	11.9	11.6	3966	N	CRAT MO	61.3	79.7
8056	118.0 65235	105.5 22803	0.055 4	112.96	5.35	4.62	3.46	6899	N	CRAT MO	16.1	20.9
8060	138.8 48559	111.6 33394	0.085 2	159.93	6.36	7	8.78	6956	N	CRAT MO	22.7	29.5
8102	53.28 11105	193.9 87653	0.057 8	108.12	7.5	7.13	8.51	4866	N	CRAT MO	15.4	20.0
8103	52.14 49923	194.4 25101	0.071 9	157.03	4.35	7.22	8.27	4867	N	CRAT MO	22.3	29.0
8131	58.57 25389	174.8 21458	0.094	226.95	5.94	6.99	7.41	4640	N	CRAT MO	32.2	41.9
8132	62.26 00978	176.4 57248	0.166	345.87	11.3	9.64	7.52	4629	N	CRAT MO	49.1	63.9
8185	126.7 59262	171.6 63919	0.169	420.77	5.85	9.77	7.19	3862	N	CRAT MO	59.8	77.7
8204	139.0 0558	142.5 40151	0.32	522.08	10.5	10.3	10	3583	N	CRAT MO	74.2	96.4
2057a	99.53 10306	164.7 36658	0.152	0	9.6	11	25.2	4550	Y	CRAT MO	0.0	0.0
2057b	99.32 44818	164.6 40394	0.125	0	9.49	14.5	12.7	4549	Y	CRAT MO	0.0	0.0
2057c	99.37 02506	165.6 58545	0.003 46	0	1.48	4.09	4.33	NA	Y	CRAT MO	0.0	0.0
2070a	50.60 03473	120.1 03453	0.368	405.02	10.9	18.1	17.5	4181	N	CRAT MO	57.5	74.8
2070b	50.63 02982	120.8 40933	0.046 8	88.82	2.83	7.14	9.22	4182	N	CRAT MO	12.6	16.4
2345a	64.39 12717	182.3 98076	0.309	346.92	9.33	16.2	22.6	4617	N	CRAT MO	49.3	64.1
2345b	64.09 17905	182.4 74211	0.094 4	69.7	8.74	11.1	2.16	4618	N	CRAT MO	9.9	12.9
8057b	118.1 59162	105.3 38662	0.197	279.78	9.24	9.88	9.75	6898	N	CRAT MO	39.8	51.7
8	123.8 5473	109.8 21824	35.11 4	6292.2 8	28.6	118	76	6931	N	FRAX EX	894.1	1162. 3
10	117.7 31667	117.4 13302	20.63 9	4004.2 8	28.6	102	93.4	3414	N	FRAX EX	569.0	739.6
206	109.1 02747	169.6 02505	4.278	2142.8 6	21.4	55.1	37.3	3894	N	FRAX EX	304.5	395.8
267	68.75 68718	197.3 93548	1.88	1062.6 3	22.4	37.1	30.3	4939	N	FRAX EX	151.0	196.3
568	111.1 50038	167.4 85135	1.565	696.56	21.3	31.4	34.4	3896	N	FRAX EX	99.0	128.7
664	100.5 78464	198.9 95809	2.459	1033.3 7	22.5	35.2	35.2	4985	N	FRAX EX	146.8	190.9
725	105.0 87591	105.7 6439	1.628	536.6	22.4	28.4	27.2	6877	N	FRAX EX	76.2	99.1
853	115.5 75313	167.8 43408	2.015	738.16	22.3	41.7	41.4	3902	N	FRAX EX	104.9	136.3
937	109.4 86962	108.0 21276	1.27	550.76	22.1	24.5	24.4	6878	N	FRAX EX	78.3	101.7
940	104.8 94913	145.2 01551	4.058	1670.3	23.6	44.2	44.6	4229	N	FRAX EX	237.3	308.5
979	103.3 347	109.0 90832	1.249	467.67	24.3	30.7	30.5	3407	N	FRAX EX	66.4	86.4
1016	126.0 79582	188.0 41656	1.418	716.81	21.3	30.4	23.3	3950	N	FRAX EX	101.8	132.4
1275	134.8 85085	120.4 99298	0.218	113.44	15.7	12.6	12.6	3445	N	FRAX EX	16.1	21.0
1302	100.9 70055	190.0 7245	2.425	1131.3 7	21.9	37.1	38.9	4981	N	FRAX EX	160.8	209.0
1361	126.8 68404	120.4 48569	1.138	414.48	23.4	21.8	21.2	3425	N	FRAX EX	58.9	76.6
1495	118.8 79717	102.6 79119	0.739	231.72	21.3	20.8	20.7	6900	N	FRAX EX	32.9	42.8
1587	120.7 81053	124.7 94804	0.842	371.87	22.4	19.2	19	3417	N	FRAX EX	52.8	68.7

1772	132.8 99631	124.8 97473	0.25	280.24	16.7	15	14.8	3437	N	FRAX EX	39.8	51.8
1776	117.9 44918	185.1 20445	2.511	1399.1	22.2	36.7	37.1	3887	N	FRAX EX	198.8	258.4
1877	135.2 76639	100.6 8228	0.501	308.28	16	16.9	17.2	6964	N	FRAX EX	43.8	56.9
2089	128.6 74993	117.0 91169	0.159	106.21	15.7	11.3	9.85	3427	N	FRAX EX	15.1	19.6
2149	47.75 37637	189.9 02402	0.059 7	87.63	8.58	8.57	2.84	4855	N	FRAX EX	12.5	16.2
2172	68.87 68179	174.9 44213	0.252	314.48	13.6	11	10.6	4636	N	FRAX EX	44.7	58.1
2317	138.8 75304	139.6 62459	0.224	258.85	15.3	10.9	11.1	3585	N	FRAX EX	36.8	47.8
8016	129.8 74428	111.2 00854	0.093 1	193.55	6.84	6.18	4.18	6952	N	FRAX EX	27.5	35.8
8027	131.4 25174	120.2 63233	0.926	349.75	22.6	24.3	24.2	3435	N	FRAX EX	49.7	64.6
8040	101.2 41322	103.8 14902	0.142	45.28	7.76	16.2	16.3	6875	N	FRAX EX	6.4	8.4
8043	102.4 32052	105.8 28573	0.112	154.41	11.3	8.53	4.39	6876	N	FRAX EX	21.9	28.5
8058	136.9 33943	121.8 0476	0.215	137.5	16	12.5	11.6	3444	N	FRAX EX	19.5	25.4
8065	97.12 00595	121.2 89118	0.020 1	40.19	6.38	4.13	2.87	4215	N	FRAX EX	5.7	7.4
8108	113.1 72388	186.2 01465	0.052 3	114.69	7.75	6.44	7.65	3889	N	FRAX EX	16.3	21.2
8129	60.31 98965	186.2 23075	0.378	271.69	9.56	19.3	21.9	4620	N	FRAX EX	38.6	50.2
8146	137.6 13606	125.2 75771	0.044 3	84.87	9.01	5.57	6.85	3442	N	FRAX EX	12.1	15.7
8162	102.2 78578	141.2 20869	0.697	201.94	23.3	21	19.3	4227	N	FRAX EX	28.7	37.3
8178	137.2 14846	177.6 58581	0.154	144.35	10.8	13.4	12.2	3873	N	FRAX EX	20.5	26.7
8208	122.3 38135	126.0 83701	0.076 9	104.38	9.01	8.6	8.96	3418	N	FRAX EX	14.8	19.3
8209	121.8 5404	133.7 27878	0.008 86	24.64	6.31	3.93	0.85	3617	N	FRAX EX	3.5	4.6
8210	119.4 83085	133.7 96731	0.011 7	15.36	3.81	4.51	3.54	3618	N	FRAX EX	2.2	2.8
8211	119.6 26298	130.8 00149	0.006 77	10.69	4.2	4.46	1.18	3619	N	FRAX EX	1.5	2.0
8215	131.3 87378	134.6 85341	0.006 69	9.8	2.15	4.21	2.41	NA	N	FRAX EX	1.4	1.8
8216	133.0 63952	136.7 01263	0.018	38.49	5.6	4.64	2.97	NA	N	FRAX EX	5.5	7.1
8217	132.9 05796	139.1 45571	0.013	22.47	4.74	4.66	3.02	NA	N	FRAX EX	3.2	4.2
8218	137.7 95899	135.7 96011	0.038 2	60.81	8.02	5.8	6.52	3587	N	FRAX EX	8.6	11.2
8221	135.0 32055	137.5 22657	0.026 6	47.66	4.74	5.79	5.09	NA	N	FRAX EX	6.8	8.8
8224	127.5 73665	122.5 72953	0.532	254.21	22.3	18.4	17.7	3424	N	FRAX EX	36.1	47.0
9106	43.29 54605	193.6 68512	0.078 1	93.72	9.3	9.73	8.12	4848	N	FRAX EX	13.3	17.3
1268a	107.6 12482	163.1 23627	1.008	622.18	20	24.5	nan	3674	N	FRAX EX	88.4	114.9
1268b	107.9 5015	163.4 63467	2.372	1365.8 6	19.9	38.7	35.8	3673	N	FRAX EX	194.1	252.3
2024a	132.3 15817	114.8 92278	0.013	0	5.86	5.47	4.21	3430	Y	FRAX EX	0.0	0.0
2024b	132.1 67597	114.8 26114	0.028 2	35.7	7.24	6.21	4.47	3429	N	FRAX EX	5.1	6.6
2310a	108.0 76739	101.6 41404	1.593	508.49	22	33.4	40	6883	N	FRAX EX	72.2	93.9
2310b	107.9 31583	101.9 33388	0.876	335.7	20.7	19.3	22	6884	N	FRAX EX	47.7	62.0
554	75.84 64664	104.3 66084	0.685	0	10.9	32.3	31.7	NA	Y	NA	0.0	0.0

8010	111.6 63198	117.0 72114	0.285	260.75	15	13	12.7	NA	N	NA	37.0	48.2
8033	67.86 30694	126.5 21119	0.028 5	9.03	8.06	8.01	8.09	NA	N	NA	1.3	1.7
8036	43.40 12207	140.7 86865	0.002 87	0	1.09	2.87	8.09	NA	Y	NA	0.0	0.0
8080	103.6 21995	130.1 4032	0.025 5	2.21	2.11	11.4	12	NA	N	NA	0.3	0.4
8085	41.06 9552	178.1 23098	0.018 3	10.12	8.92	6.38	4.52	NA	N	NA	1.4	1.9
8089	43.87 14068	183.2 23908	0.019 3	11.95	6.59	5.08	6.76	NA	N	NA	1.7	2.2
8097	52.56 54442	189.8 18149	0.013 4	37.29	4.82	4.67	5.65	NA	N	NA	5.3	6.9
8112	102.5 59301	196.0 29695	0.007 44	11.83	4.73	3.5	3.72	NA	N	NA	1.7	2.2
8153	89.38 8262	162.8 0125	0.052	82.98	7.3	6.45	6.3	NA	N	NA	11.8	15.3
8154	89.25 26048	159.9 66917	0.020 2	54.4	6.05	4.76	4.06	NA	N	NA	7.7	10.0
8156	95.27 42353	157.7 49246	0.041 9	63.49	8.27	7.66	6.88	NA	N	NA	9.0	11.7
8157	97.19 14691	158.0 52769	0.114	85.82	10.8	13.1	8.78	NA	N	NA	12.2	15.9
8158	96.67 6581	156.0 63019	0.011 2	9.64	6.63	5.61	3.22	NA	N	NA	1.4	1.8
8165	109.3 34979	145.3 85544	0.043 8	76.71	9.79	7.5	4.21	NA	N	NA	10.9	14.2
8170	106.1 60315	149.8 47098	0.034 6	51.5	9.43	5.99	8.09	NA	N	NA	7.3	9.5
8189	138.2 21841	160.5 88292	0.058 8	13.1	9.67	13.4	16.7	NA	N	NA	1.9	2.4
8191	132.2 04519	165.6 09673	0.025 8	31.76	7.72	6.88	1.4	NA	N	NA	4.5	5.9
8212	126.5 45485	128.6 86235	0.048 2	97.67	5.39	5.51	1.03	NA	N	NA	13.9	18.0
9087	56.02 53777	113.5 27082	0.014	0	1.43	0.5	12.6	NA	Y	NA	0.0	0.0
9097	62.32 8344	123.6 44925	0.015 8	0	2.54	9.97	10.3	NA	Y	NA	0.0	0.0
8026a	58.24 46434	121.0 29591	0.016 3	22.36	3.86	6.14	6.33	NA	N	NA	3.2	4.1
8026b	58.27 9823	120.7 99233	0.019 6	14.68	2.94	6.92	5.72	NA	N	NA	2.1	2.7
8029a	42.61 50194	106.2 40906	0.018 1	2.13	1.99	11.9	5.35	NA	N	NA	0.3	0.4
8029b	42.38 07051	106.3 89034	0.002 62	1.38	0.62	0.5	3.52	NA	N	NA	0.2	0.3
8047a	99.65 84205	105.8 13935	0.042 6	97.52	5.23	5.98	3.28	NA	N	NA	13.9	18.0
8047b	99.63 92392	106.3 74773	0.163	299.67	10.7	8.19	8.5	NA	N	NA	42.6	55.4
8088c	43.56 0514	181.2 37554	0.009 99	16.8	3.17	4.54	6.4	NA	N	NA	2.4	3.1
8113a	103.7 79409	187.3 03789	0.085 6	207.68	4.73	8.44	5.05	NA	N	NA	29.5	38.4
8113b	103.3 9045	187.2 14906	0.124	287.88	8.82	8.08	6.07	NA	N	NA	40.9	53.2
8115a	100.5 75052	191.5 65543	0.121	294.38	7.67	13	11.6	NA	N	NA	41.8	54.4
8115b	99.98 76895	191.8 13984	0.078	86.42	11.3	10.9	10.2	NA	N	NA	12.3	16.0
8122a	63.91 25287	198.7 73176	0.017	0	6.78	5.72	6.08	NA	Y	NA	0.0	0.0
8122b	64.57 34927	198.8 83577	0.179	151.76	14.5	12.7	6.67	NA	N	NA	21.6	28.0
8122c	64.35 41061	198.6 69315	0.015	0	4.76	6.62	6.33	NA	Y	NA	0.0	0.0
8149a	122.0 7032	122.6 88448	0.012 7	19.65	5.97	4.72	3.94	NA	N	NA	2.8	3.6
8149b	122.3 79635	122.8 14797	0.057 5	63.09	11.8	7.71	9.52	NA	N	NA	9.0	11.7

8163a	103.9 03692	139.1 99254	0.020 3	52.46	4.42	4.59	1.77	NA	N	NA	7.5	9.7
8163b	104.6 88901	139.6 59328	0.095 7	175.61	6.8	7.5	4.5	NA	N	NA	25.0	32.4
8163c	104.6 11491	139.0 60829	0.036 5	85.52	5.56	5.38	3.13	NA	N	NA	12.2	15.8
9102b	46.21 33078	199.3 50892	0.032 7	0	4.74	10.5	10.4	NA	Y	NA	0.0	0.0
22	80.41 00038	134.5 28075	7.987	1748.2 3	22	77.4	19.2	4249	N	QUE RRO	248.4	322.9
41	76.78 66205	165.4 96382	3.885	0	16.6	66.7	58	4508	Y	QUE RRO	0.0	0.0
46	41.20 71615	134.0 04755	5.297	1239.5 2	19.2	69	62.4	4286	N	QUE RRO	176.1	229.0
74	67.60 62223	168.9 687	8.421	2927.2 6	22.7	71.3	66.9	4634	N	QUE RRO	415.9	540.7
81	133.0 52774	162.3 41695	14.28	3239.8 7	22.5	99.7	8.38	3704	N	QUE RRO	460.3	598.4
118	63.51 44291	175.0 8105	2.836	576.02	21.6	45.8	47.7	4631	N	QUE RRO	81.8	106.4
134	54.45 93103	159.3 33946	4.816	1557.2 2	22.7	56.1	52.2	4484	N	QUE RRO	221.3	287.6
135	99.02 33282	108.6 8264	5.104	929.58	22.2	55.8	51.6	4216	N	QUE RRO	132.1	171.7
163	108.0 70788	121.9 68748	7.086	1140.6 3	23.2	71.6	23.1	3392	N	QUE RRO	162.1	210.7
195	138.1 73374	133.2 82423	18.96 8	4169.3	23.4	99.4	77	3588	N	QUE RRO	592.4	770.1
225	106.0 93165	175.1 90782	2.653	45.2	10	65.5	64.3	3893	N	QUE RRO	6.4	8.3
226	122.5 2547	135.4 33454	3.137	431.59	23.2	46.3	46.5	3616	N	QUE RRO	61.3	79.7
253	140.2 68549	184.7 17295	2.793	592.58	15.6	57.2	51.6	3874	N	QUE RRO	84.2	109.5
325	92.51 75852	168.5 67025	2.784	1034.2 5	15.8	45.7	30.3	4575	N	QUE RRO	147.0	191.0
348	114.2 85917	182.0 72931	7.069	2618.8 3	18.8	78	67.2	3890	N	QUE RRO	372.1	483.7
393	116.9 21897	191.1 71798	4.609	1038.7 8	18.6	67.9	56.9	3936	N	QUE RRO	147.6	191.9
425	118.7 25049	148.3 77903	2.497	213.3	19.9	60.1	48.2	3613	N	QUE RRO	30.3	39.4
434	137.4 24604	152.2 07336	1.917	358.77	20.6	39.5	39.7	3716	N	QUE RRO	51.0	66.3
795	131.6 14698	170.4 54051	6.782	1962.4 1	24	74.4	66.4	3870	N	QUE RRO	278.8	362.5
838	83.93 92957	144.0 7524	3.658	986.36	21.2	50.8	46.5	4244	N	QUE RRO	140.1	182.2
973	89.48 78845	169.7 65514	1.631	397.24	14.6	47	44.1	4576	N	QUE RRO	56.4	73.4
1074	59.43 67909	175.1 5935	7.033	2237.4 3	22.7	69.1	64	4627	N	QUE RRO	317.9	413.3
1191	134.7 44322	193.3 54647	4.988	1075.7 1	18.6	70.6	61.1	3956	N	QUE RRO	152.8	198.7
1567	51.78 93864	181.8 48928	3.583	789.19	20.7	61.9	28.5	4653	N	QUE RRO	112.1	145.8